RECONSTRUCTING LATE HOLOCENE FLOOD RECORDS IN THE TYWI CATCHMENT

Final report for
Dyfed Archaeological Trust
for the Exploration Tywi! Project.

February 2011

Anna F. Jones, Paul A. Brewer, Mark G. Macklin and Catherine. H. Swain

Centre for Catchment and Coastal Research
Institute of Geography and Earth Sciences
Aberystwyth University
Aberystwyth
SY23 3DB

Contents

List of Figures

List of Tables

1. Introduction

1.1 Background

Long flood series are essential for understanding magnitude-frequency relationships of high-magnitude floods (Kochel and Baker, 1982; Ely et al., 1993), however, the vast majority of instrumental flood records worldwide are no longer than 50 years (Benito et al., 2004; Macklin and Rumsby, 2007), and this is also the case for most instrumental records from Welsh river catchments. Documentary or epigraphic flood records may be used to extend the record through the period before the installation of instrumentation. However, historical recording of floods has typically been concentrated in major settlements and, therefore, such records, particularly series of recorded historical flood levels, are relatively rare in Welsh catchments. Sedimentological data, recorded in sediments deposited during flood events, provide a potential means of extending instrumental and historical flood records and obtaining information about high-magnitude flood events with low annual exceedence probabilities.

The most widely used sedimentological technique for reconstructing long term flood records involves analysis of slackwater sediments in bedrock gorges, most commonly found in semi-arid or arid environments (Kochel and Baker, 1982; Baker et al., 1983; Sheffer et al., 2008). In temperate catchments flood records have been derived from boulder berms in upland areas (Macklin and Rumsby, 2007), and from layers of sand or gravel in floodplain sediments (Knox, 1987, 1993, 2003; Macklin et al., 1992; Moores et al., 1999; Goman and Leigh, 2003), identified by textural reversals in sedimentary sequences. However, it has not been possible to use these methods to reconstruct flood records from finer-grained silty floodplain sediments without visible stratigraphy, which are widespread in temperate regions including Wales. Development of new techniques for reconstructing flood records from this type of floodplain environment is therefore required and is the subject of this report.

1.2 Aims and objectives

This report aims to provide ‘proof-of-concept’ for a recently developed method of reconstructing long flood histories using high-resolution analysis of floodplain sedimentary sequences, which is suitable for application in catchments of the type found in Wales. To this end it has the following objectives:

1. To establish the recent history of flooding, and of variations in flood magnitude, through analysis of instrumental flood records;
2. To describe the methods used in reconstructing long flood records from floodplain sedimentary sequences;
3. To demonstrate that the grain size proxies employed are suitable for use at the study sites;
4. To produce long dated flood records from floodplain sediment sequences within the Tywi catchment, which can be used to investigate relationships between flooding and climate;
5. To compare the sedimentary flood record with available historical flood records, in terms of length and type and utility of the information provided.

1.3 Structure of the report

This report consists of six sections, including this introduction. Section 2 describes the Tywi catchment and site investigated as part of this research. Section 3 presents flow data from three gauging stations within the Tywi catchment. Recent (decadal-scale) variations in flood magnitude are described and their effects on the results of flood frequency analysis are assessed. Section 4 summarises the available historical flood data for the Tywi catchment. Section 5 presents flood records constructed using high-resolution Itrax core scanning of sedimentary sequences from Abermarlais. Section 6 summarises the main findings of the study and suggests lines of enquiry for further research.

2. The Tywi catchment and Abermarlais study site

The Afon Tywi, in south-west Wales, is 114 km in length and has a catchment area of 1373 km^2. The catchment rises to 802 m above Ordnance Datum in Black Mountain, on its southern boundary. The catchment is predominantly underlain by mudstones, siltstones and greywackes of Ordovician and Silurian age but at the southern margin of the catchment Devonian sandstones (Old Red Sandstone) and Carboniferous limestone crop out. Grassland, used either for hill-farming, livestock farming or dairying, is the predominant land cover type within the catchment and there is also a significant proportion of woodland. Arable land and urban areas constitute relatively small percentages of catchment land cover.

Instrumental flow records were available for gauges at Dolau Hirion, upstream of the Exploration Tywi! study reach, and at Ty Castell and Capel Dewi, both downstream of the Exploration Tywi! study reach (Figure 1). Reconstruction of the sedimentary flood record was undertaken for the Abermarlais site. This is located at the upstream end of the Exploration Tywi! study reach at c. 42 m O.D. The Tywi in this reach has a low sinuosity and a gradient of 0.013 m m^{-1}. Floodplain sediments are characterised by relatively thick, in comparison to sites downstream, sequences of fine-grained (silt- and clay-dominant) sediment derived mainly from Lower Palaeozoic mudstones. The site lies upstream of the confluence of the Tywi with the Sawdde, which is the main source of sediment derived from the Old Red Sandstone to the Tywi. The floodplain sediments at Abermarlais also contained significant quantities of organic material suitable for radiocarbon dating, which could be used to establish the age of the reconstructed flood record.

3. Analysis of instrumental flood records from the Tywi catchment

3.1 Introduction

This section presents an analysis of variations in flood magnitude and frequency in the gauged records from the Tywi catchment. This represents the first part of the process involved in building up a long record of flooding which may be used to constrain flood magnitude-frequency relationships, particularly of those events with low annual exceedence probabilities. Due to the relatively short length of the available records, analysis of instrumental records provides most certain information about relatively frequent flood events. Further information, from historical or palaeoflood data, is therefore required to understand the magnitude-frequency relationships of rare, high-magnitude flood events. However, flood events of sufficient magnitude to be identified within a palaeoflood record may have occurred during the period of historical recording. The combination of instrumental and palaeoflood data may then provide more useful information about flood events of that magnitude than can be obtained from either record in isolation. For this reason this section contains, first, and assessment of the sources of instrumental data available for analysis, second, and analysis of temporal variations in annual maximum flood magnitudes within the Tywi catchment and, third, flood frequency analysis of available data.

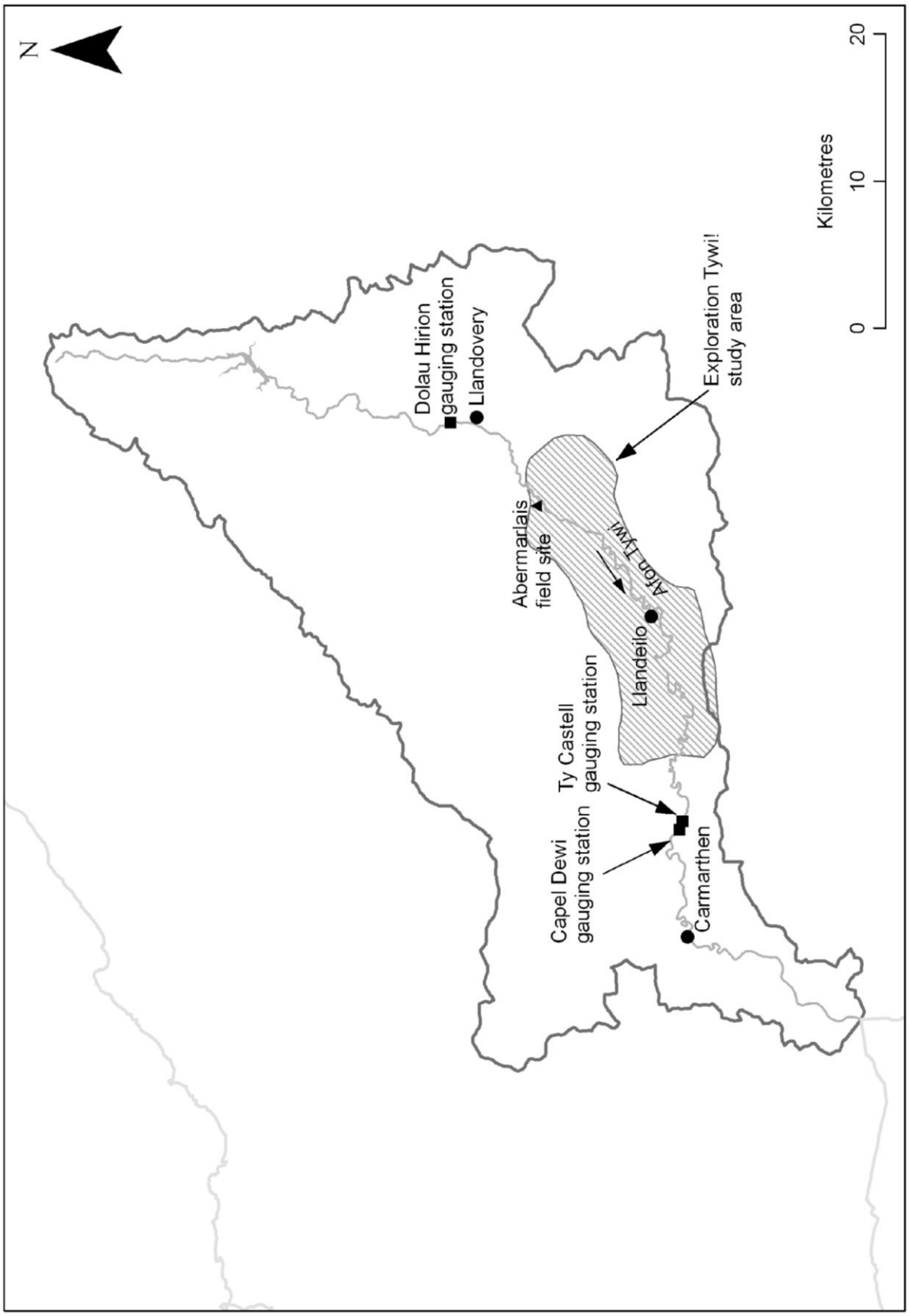

Figure 1: The Tywi catchment, south Wales, showing the locations of the Exploration Tywi! study area, the principal towns, the three gauging stations and the Abermarlais field site.

3.2 Methods and data sources

Analysis of the gauged records was based on water years (starting October 1st) since winter flooding dominates the regime. Water years were labelled using the calendar year in which they begin, following the convention used by Robson and Reed (1999). Flood frequency analyses were carried out using the return period approach described by Gumbel (1958). The data were plotted on log-normal axes (Dunne and Leopold, 1978) using the Weibull formula to determine plotting positions.

Data from the Dolau Hirion, Ty Castell and Capel Dewi flow gauges on the Afon Tywi were analysed (Figure 2). The Dolau Hirion gauge is a velocity-area station draining a catchment of 232 km^2 which contains the Llyn Brianne reservoir. The gauge's primary purpose is flood warning (Environment Agency, 2010). The Ty Castell and Capel Dewi stations, in the lower part of the catchment, are located only 0.6 km apart but have different purposes: the primary purpose of the Ty Castell gauge is flood flow gauging while that of the Capel Dewi gauge is monitoring abstraction (Environment Agency, 2010). This means that the Ty Castell gauge is the more appropriate for this analysis. However, there are no daily mean or daily maximum flow data for this gauge for the years 1984 to 1998. For this reason data from both gauges are included in the analysis. The Ty Castell gauge is a velocity-area station in a straight stable reach with rock at the right bank (Environment Agency, 2010). The Ty Castell gauge is a flat V weir set in a Crump profile flanking section (Environment Agency, 2010). High-magnitude flows at this site spill over the right bank and bypass the station (Environment Agency, 2010).

Three types of flow data were available from the Environment. These were the daily mean flow series, the daily maximum flow series and the HiFlows-UK annual maximum series (downloadable from the online HiFlows-UK archive), which records flood peak discharges (Environment Agency, 2010). Record lengths for each type of record at the three gauging stations are shown in Table 1.

Table 1: Record lengths of available daily mean flow, daily maximum flow and HiFlows-UK annual maximum series for the selected flow gauges.

	Dolau Hirion	**Ty Castell**	**Capel Dewi**
Gauging station established	25/04/1968	01/01/1958	01/02/1958
Daily mean flows (water years)	1968-2008	1958-1983 and 1999-2009	1974-2009
Daily maximum flows (water years)	No record	1981-1983 and 1999-2009	1981-2009
HiFlows-UK annual maximum data (water years)	1967-2007	1957-2007	1957-2007*

* HiFlows-UK data for 1957-1973 water years at Capel Dewi have been derived from data from the Ty Castell gauge (Environment Agency, 2010).

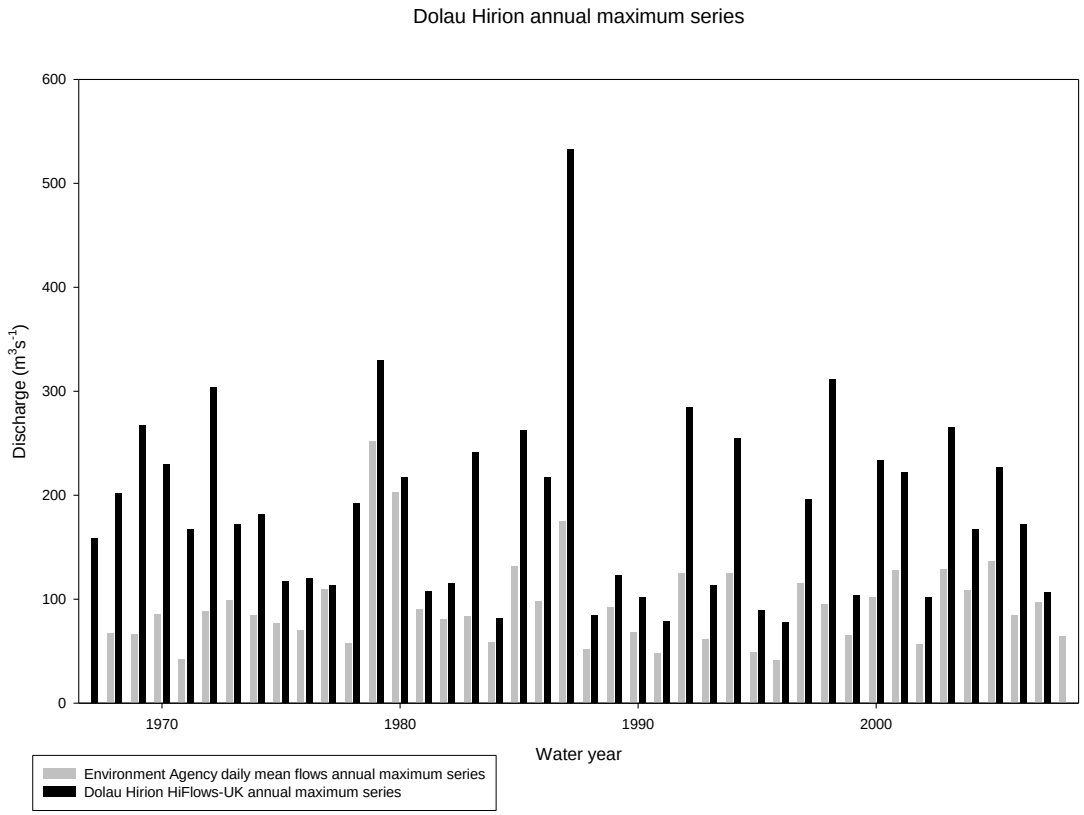

Figure 2: Annual maximum series derived from daily mean flow data and HiFlows-UK data for the Dolau Hirion flow gauge.

It would be expected that for each water year the annual maximum series derived from daily mean flows would be the lowest of the available values and that those derived from the daily maximum flows and the HiFlows-UK annual maximum series should be identical. Exceptions to this may be found during years for which data in any one data series are incomplete, for example, the water year in which recording of the daily maximum flow data began. Figures 2 to 4 compare the annual maximum series derived from each available data source for each of the three gauges.

At the Dolau Hirion gauge, the annual maximum flood discharge from the HiFlows-UK archive always exceeds that derived from the mean daily flow record, as expected (Figure 2). In many years the difference between the two values exceeds 100 m^3s^{-1}, which is large considering that the annual maximum mean daily flows are normally less than 100 m^3s^{-1}. The relative magnitudes of the annual maximum floods vary considerably between the two series: the three largest events in the record derived from the mean daily flow data occurred in 1979 (252 m^3s^{-1}), 1980 (203 m^3s^{-1}) and record the 1987 event (553 m^3s^{-1}) was the largest, followed by those of 1979 (330 m^3s^{-1}) and 1998 (312 m^3s^{-1}).

At the Ty Castell gauge, the annual maximum flood discharge derived from the mean daily flow data is normally exceeded by that from the HiFlows-UK annual maximum flood archive but with two exceptions in the 1982 and 2004 water years (Figure 3). The values from the HiFlows-UK annual maximum series and that derived from the daily maximum flow data are frequently different, contrary to what would be expected. Either of the two values may be greater than the other and the maximum difference between the two values is greater than 150 m^3s^{-1}.

At the Capel Dewi gauge the annual maximum flood magnitudes derived from the daily mean flow data are frequently greater than those from the HiFlows-UK archive, contrary to what should be expected, during the mid to late1970s and also in a number of cases during the 1980s. As at the Ty Castell gauge, there are substantial differences between the annual maximum series derived from daily maximum flow data and that from the HiFlows-UK archive. In some cases the HiFlows-UK value is the greater and in others that from the daily maximum flow data.

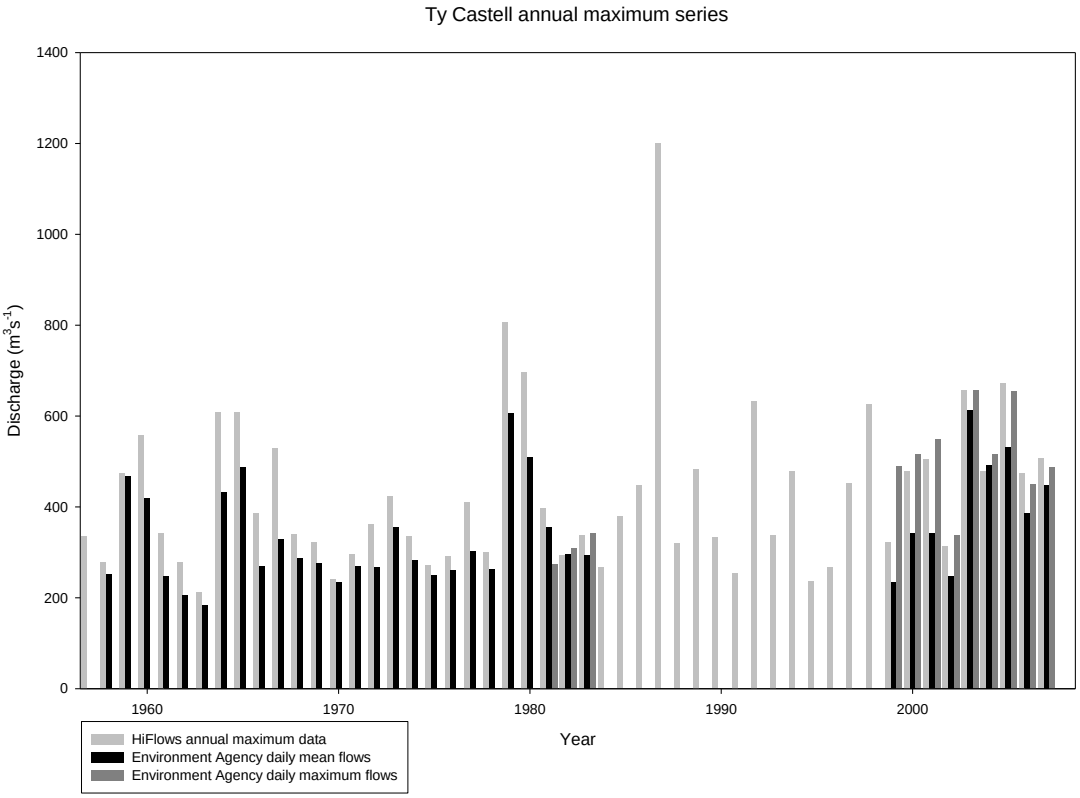

Figure 3: Annual maximum series derived from daily mean flow data, daily maximum flow data and data from the HiFlows-UK archive for the Ty Castell flow gauge.

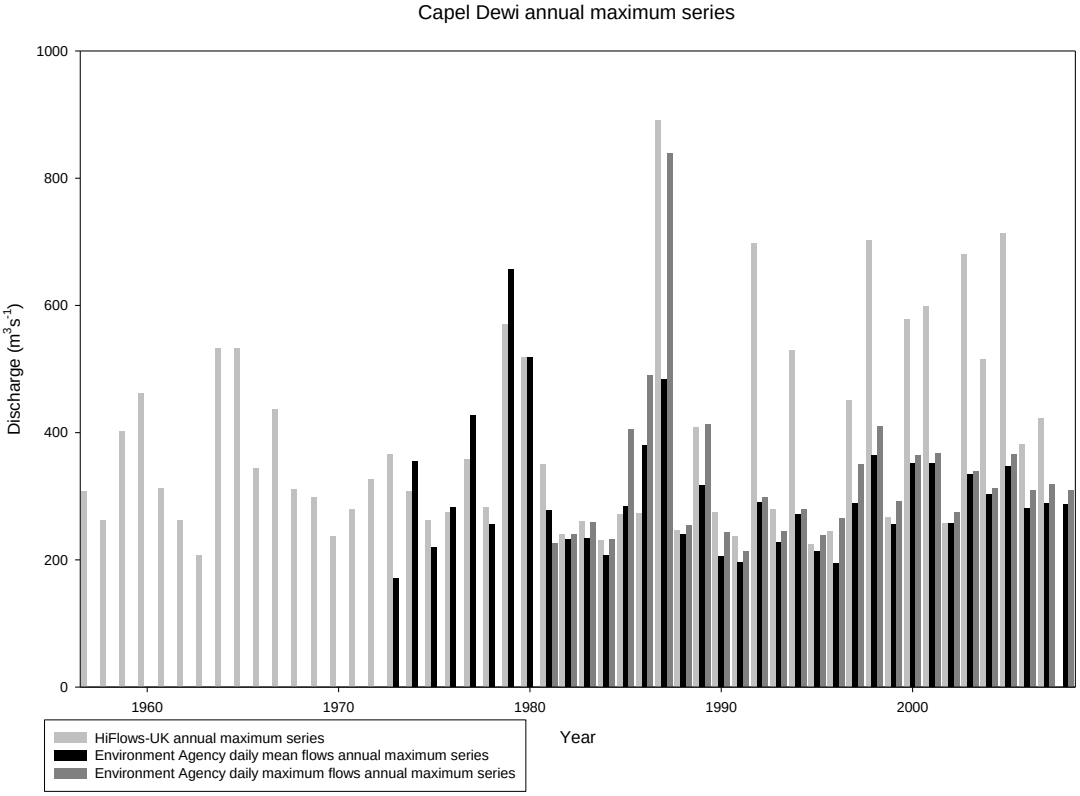

Figure 4: Annual maximum series derived from daily mean flow data, daily maximum flow data and data from the HiFlows-UK archive for the Capel Dewi flow gauge.

1987 (175 m^3s^{-1}) respectively, whereas in the HiFlows-UK annual maximum flood

In 7 cases during the 1990s and 2000s the HiFlows value exceeds that from the daily maximum flow data by more than 200 m^3s^{-1}. The largest of these discrepancies is 398 m^3s^{-1} during the 1992 water year. As the values in the two series were recorded on the same day this difference is not due to missing flow data causing the two data series to record different events.

Inconsistencies between the various data sets for the same flow gauge may lead to the generation of significantly different flood frequency curves for the same record. The differences between the flood frequency curves produced will be most significant in cases where either the variation in reported flood magnitudes is greatest or where a large number of flood events are absent from one of the data sets. In some cases the differences between records from the same gauge could have far-reaching implications in planning and engineering applications. The lack of information on how discrepancies in flood magnitudes might have resulted means that it is currently impossible to determine which data series constitutes the most accurate record of flooding at each site without further information.

3.3 Variations in flood magnitude

The annual maximum flood series have been plotted for each data source for the three gauging stations and the pattern of variation smoothed using 5-year (cf. Higgs, 1987; Longfield and Macklin, 1999) and 9-year moving averages (Figures 5 to 7).Temporal variations in the magnitude of the annual maximum flood are apparent at all three stations.

At the Dolau Hirion gauge the mean daily flow data show an increase in annual maximum flood discharge from the beginning of the record, reaching a peak in 1979-1980. This was followed by a decrease in flood magnitudes with a minor peak at c. 1985-1987. Annual maximum flood magnitudes were generally lower during the early to mid 1990s and then increased again towards the end of the record. The pattern of variation shown by the HiFlows-UK (instantaneous annual maximum) data is somewhat different with a peak in annual maximum flood magnitude around 1970 followed by a decrease to the mid 1970s. There is a minor peak in the late 1970s to early 1980s but the most prominent peak in the record occurs at 1985-1987. This is followed by a decrease to the mid 1990s and an increase towards the end of the record. The

difference in the magnitude of the annual maximum flood discharges between the two datasets is striking: in the daily mean flow data the largest flood peak is a little over 250 m^3s^{-1} while in the HiFlows-UK data the magnitude of the greatest annual maximum flood peak is in excess of 500 m^3s^{-1}. In this small, rapidly responding upland catchment it appears that there may be large differences between daily mean and maximum flows.

At the Ty Castell gauge there are long gaps (1984-1998) in the annual maximum flood records derived from both the daily mean and daily maximum flow records, which make it difficult to identify temporal variations in the magnitude of the annual maximum flood. The short record derived from the daily maximum flow series shows that the greatest annual maximum flood peaks occurred in the 2003 and 2005 water years. The flood peaks recorded in the 1981-1983 water years are smaller than the majority of those which occur during the period 1999-2009. The annual maximum flood record derived from the daily mean flow series contains a peak in the early part of the record with the greatest annual maximum flood event occurring in the 1965 water year.

Relatively low annual maximum flood peaks were recorded during the early to mid 1970s followed by an increase to a peak in 1979-1980. In the most recent part of the record there is a peak at c. 2003-2005, corresponding to that in the daily maximum flow record. The HiFlows-UK record is the only one which covers the entire period and this indicates that the annual maximum flood event in the 1987 water year dwarfs every other annual maximum flood discharge in the record. The pattern of variation in the early part of the record is similar to that in the annual maximum series derived from the daily mean flow record, although the magnitude of the instantaneous maximum discharges is 100-200 m^3s^{-1} greater for the larger events in this period. The later part of the record shows a similar pattern to that recorded at Dolau Hirion, namely a decrease in mean annual maximum flood magnitudes to the early to mid 1990s followed by an increase to the end of the record.

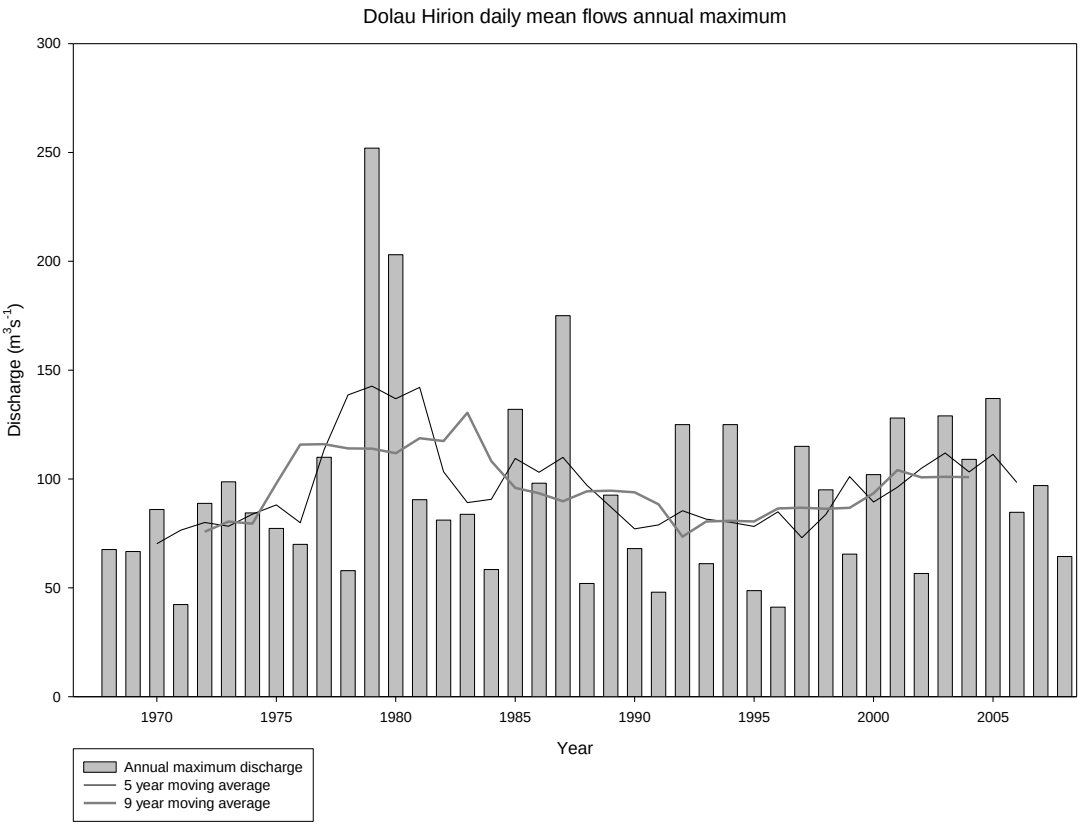

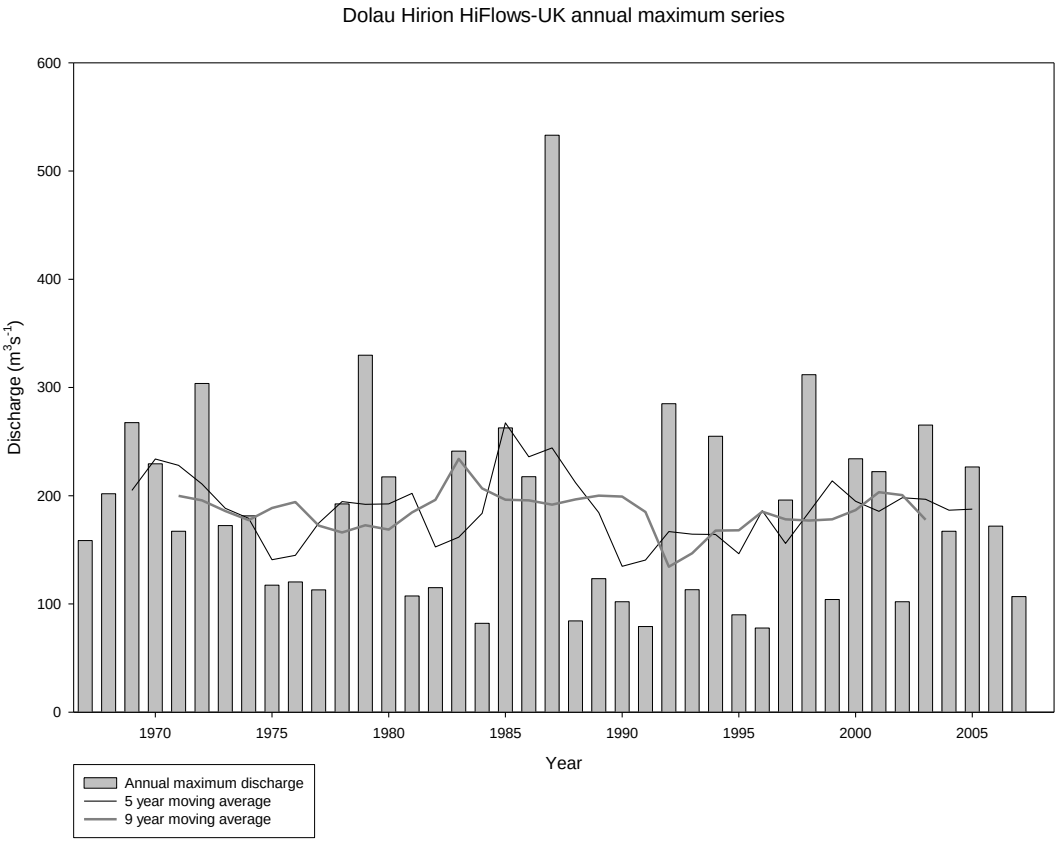

Figure 5: Temporal variations in the magnitude of the annual maximum flood at Dolau Hirion. Flood magnitudes are derived from daily mean flow data (top) and the HiFlows-UK archive (bottom).

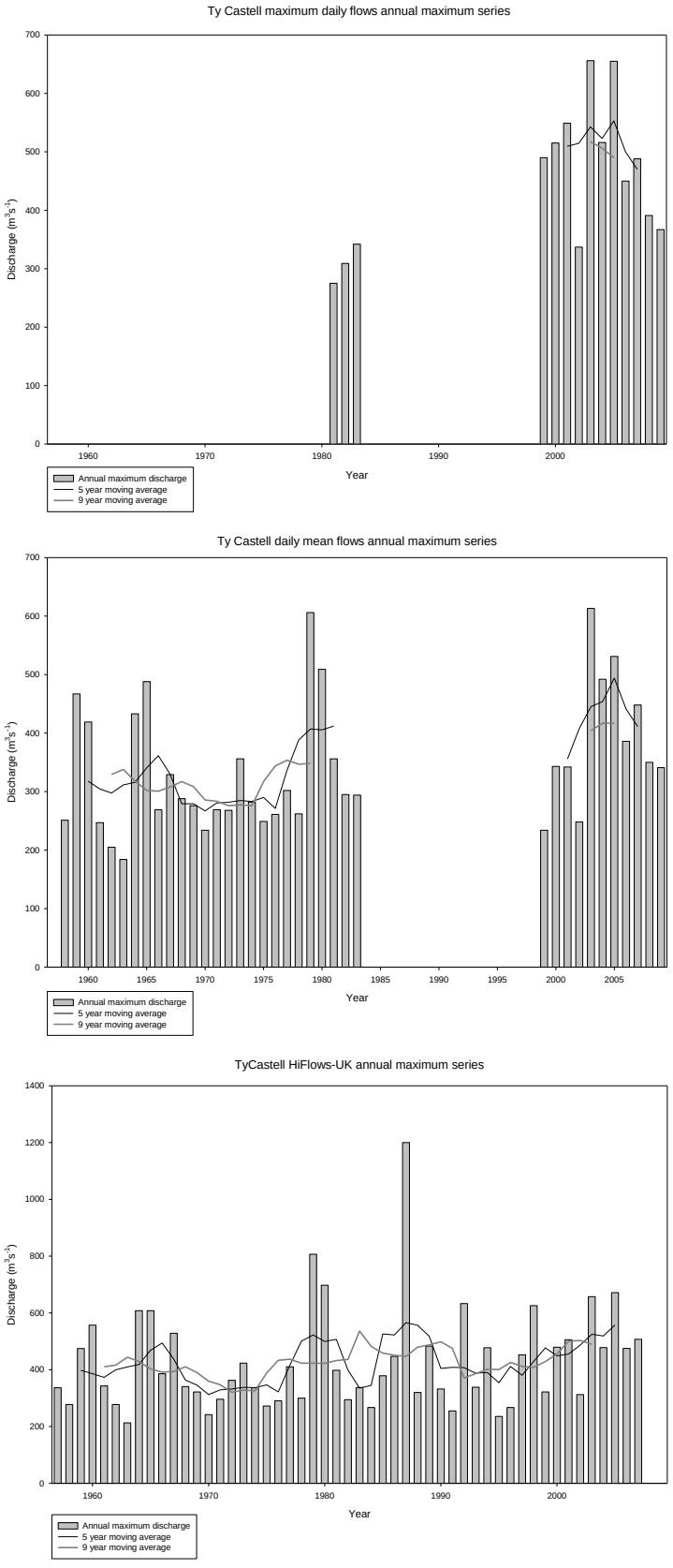

Figure 6: Temporal variations in the magnitude of the annual maximum flood at Ty Castell. Flood magnitudes are derived from daily maximum flow data (top), daily mean flow data (middle) and the HiFlows-UK archive (bottom).

At the Capel Dewi gauge the annual maximum flood record derived from the maximum daily flow record shows a peak at 1985-1989 and a lesser peak at 1998-2000 with a slight decrease towards the end of the record. The longer annual maximum flood record derived from daily mean flows records a peak in mean annual maximum flood magnitude at 1977-1980. The peak in mean annual maximum flood magnitudes at this time is larger than that recorded at 1985-1988 in the daily mean flow record. The pattern of variation in mean annual maximum flood magnitude recorded in the HiFlows-UK record is somewhat different to those in the other two records. This shows that the greatest peak in mean annual maximum flood magnitude occurred in the most recent part of the record at 2003-2005 and that there is little decrease after the peak at 1987, as a result of the number of events with discharges greater than 500 m^3s^{-1} recorded during the 1990s and 2000s. In addition to the earlier peak at 1979, which is of a similar magnitude to that at 1987, there is also a peak in the mid 1960s, similar to that recorded at Ty Castell.

The differences between the annual maximum flood records produced from the different data sources for the three gauges show that caution is required when interpreting the data. This is also required due to the relatively short length of the records available. However, none of the records produced show a consistent trend in flood magnitude through the record. The HiFlows-UK record for the Capel Dewi gauge does show a sustained increase in annual maximum flood magnitude in the latter part of the record but this is not replicated in the other records at this site and this gauge is also less suitable than the upstream Ty Castell gauge for the assessment of flood flows. There is likewise no evidence for a step-change, either increasing or decreasing, in flood magnitude in any of the records from the three gauges. Throughout large parts of the record the 5-year and 9-year moving averages fluctuate within relatively narrow limits suggesting that the observed pattern of annual maximum flood peaks is a result of stochastic variation about a mean that has not changed significantly. The clustering of high-magnitude flood annual maximum events temporarily increases flood magnitude and inter-annual variability in certain parts of the records, most noticeably at c. 1960, c. 1965, c. 1979-1980, c. 1985-1987 and c. 2005. This suggests that floods in the Tywi catchment may not be the outcome of an independent and identically distributed random process (cf. Jain and Lall, 2000; 2001), which would violate one of the key assumptions underpinning statistical flood frequency analysis. However, with such a small amount of data this is difficult to verify.

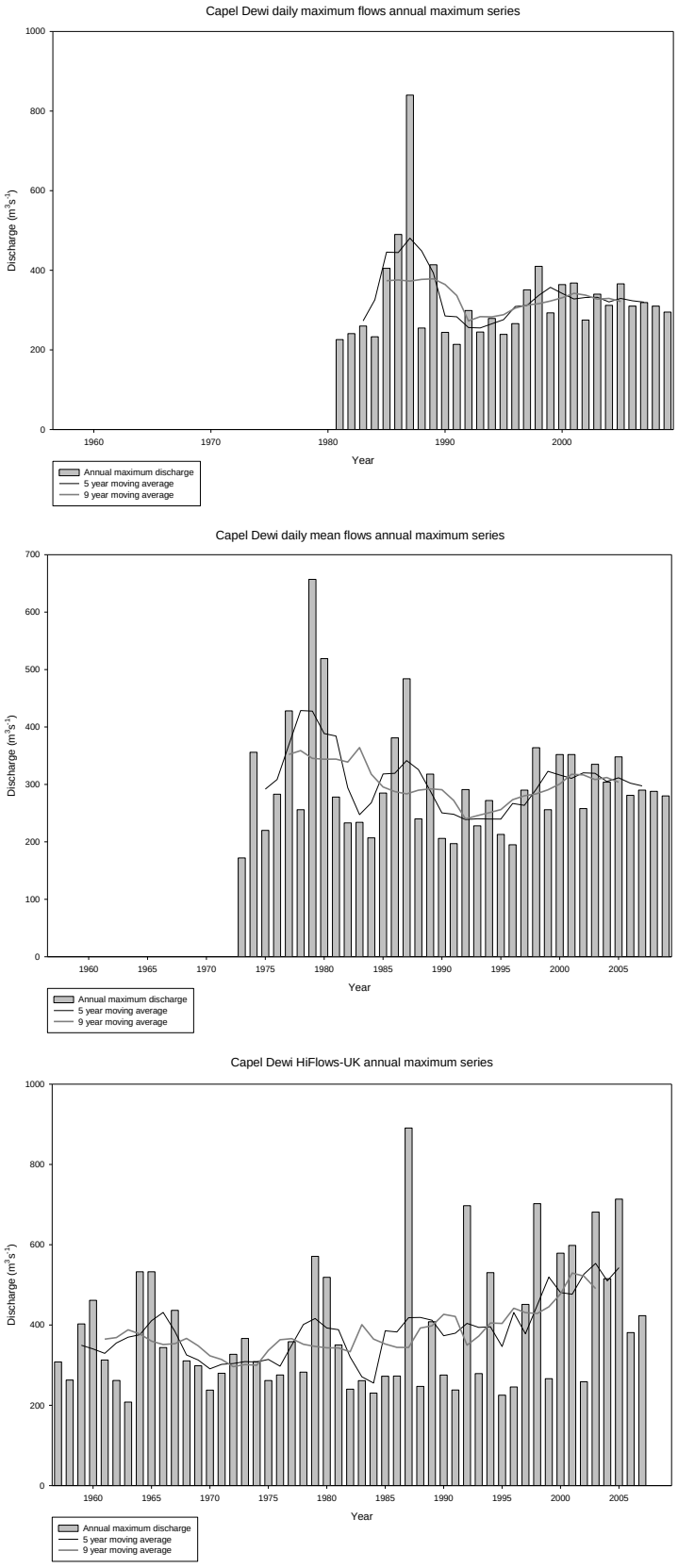

Figure 7: Temporal variations in the magnitude of the annual maximum flood at Capel Dewi. Flood magnitudes are derived from daily maximum flow data (top), daily mean flow data (middle) and the HiFlows-UK archive (bottom).

The other main assumption of statistical flood frequency analysis, that of stationarity of the mean, appears to be reasonable for the data presented here, with the sole possible exception of the HiFlows-UK annual maximum flood record from Capel Dewi, but the reasons for treating this record with caution have been presented above. The results of this analysis do imply that the results of a statistical flood frequency analysis conducted on data from these gauging stations may be influenced by the particular years for which data are available for analysis.

3.4 Flood frequency analysis

Each of the annual maximum flood records from the Dolau Hirion, Ty Castell and Capel Dewi gauges were divided into sections on the basis of changes in the winter North Atlantic Oscillation index, which has been shown to be related to variations in flood magnitude in other British catchments (e.g. Macklin and Rumsby, 2007). The winter North Atlantic Oscillation index for the period from 1900 to 2009 is shown in Figure 8. The record has been divided on the basis of the 5-year mean of the winter NAO into five periods: 1957-1960, where the mean winter NAO was weakly positive; 1971-1960, when the mean was negative; 1971-1985, when the mean was generally weakly positive with a short negative episode during the late 1970s; 1986-1996, when there was a significant peak in the mean of the winter NAO; and 1997-2009, where it was generally weakly positive, with the exception of the winter of 2009-2010.

Kidson and Richards (2005) have reviewed limitations of techniques currently used in flood frequency analysis. The short length of the records analysed here, particularly of the partitioned records, reduces the confidence that can be attached to the results. For each record type and each gauge flood frequency analysis was carried out on the entire record and on the data for each of the periods defined using the NAO record.

Flood frequency analysis on the annual maximum flood record derived from the daily mean flow data at Dolau Hirion suggests that flood frequencies in different periods of the record were relatively similar, as the series fall close to each other through much of the record (Figures 9-11). However, frequent floods (annual exceedence probabilities 50 % or less) were noticeably smaller during the period from 1986 to 1996. The results indicate that the annual maximum daily mean flow exceeds 200 m^3s^{-1} in approximately

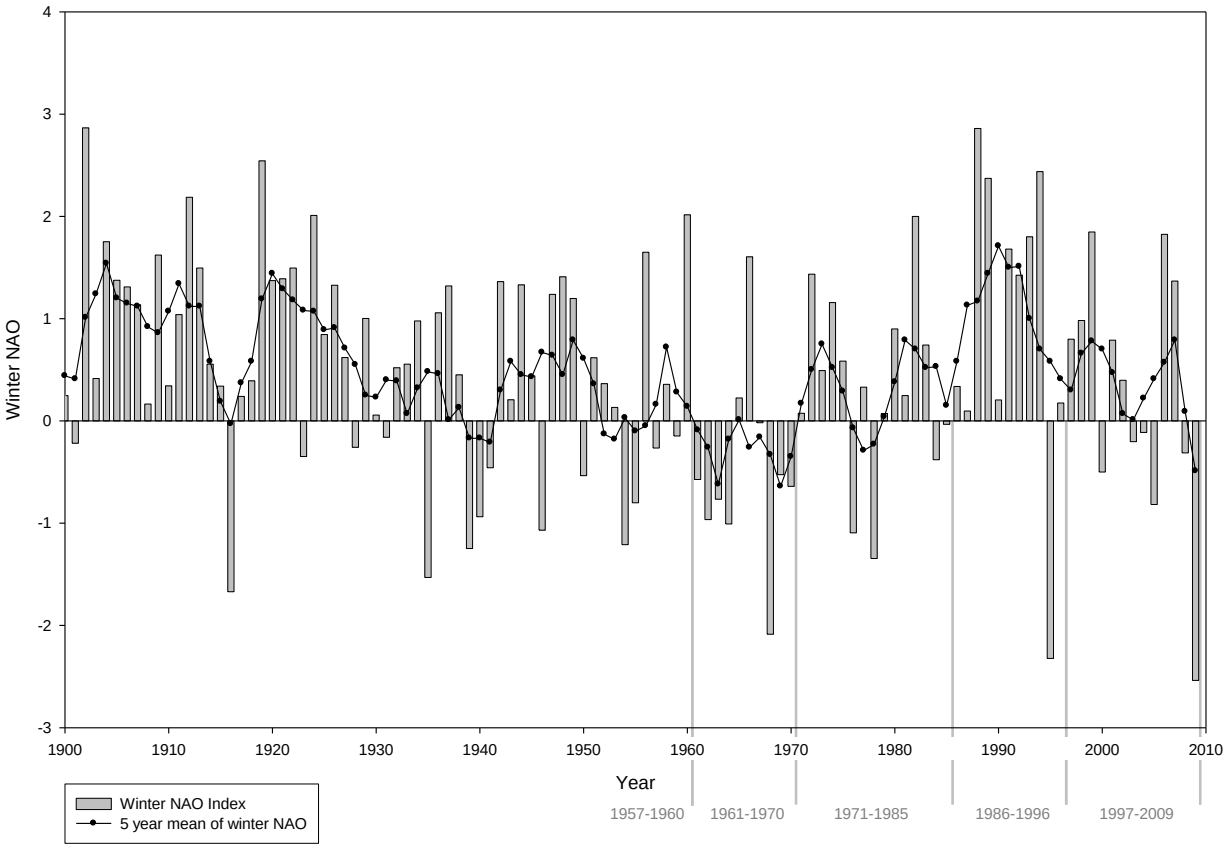

Figure 8: Variations in the winter (December-March) North Atlantic Oscillation index between 1900 and 2009. The data have been smoothed using a 5-year running mean which has been used to define five periods (below right) into which the annual maximum flood records have been divided for flood frequency analysis.

one year in 20 through the whole record. This rises to more frequently than one year in ten during the 1971-1985 period as a result of the occurrence of the two highest mean daily flows during this period. The results from the analysis of the HiFlows-UK annual maximum data are somewhat different: in each data series, except that for the 1967-1970 water years, there is a noticeable step change in the magnitudes of the annual maximum floods as the exceedence probability decreases. This occurs at between c. 70 % and 40 % annual exceedence probabilities, depending on which part of the record is analysed. This effect may result from the operation of the Llyn Brianne to contain flood flows when floodwater storage capacity is available. In the whole record the apparent reduction in flows which may be due to the operation of the reservoir occurs for floods with exceedence probabilities greater than c. 60 %. The HiFlows-UK instantaneous maximum data indicate that annual maximum flood peaks exceed 300 m^3s^{-1} approximately one year in ten.

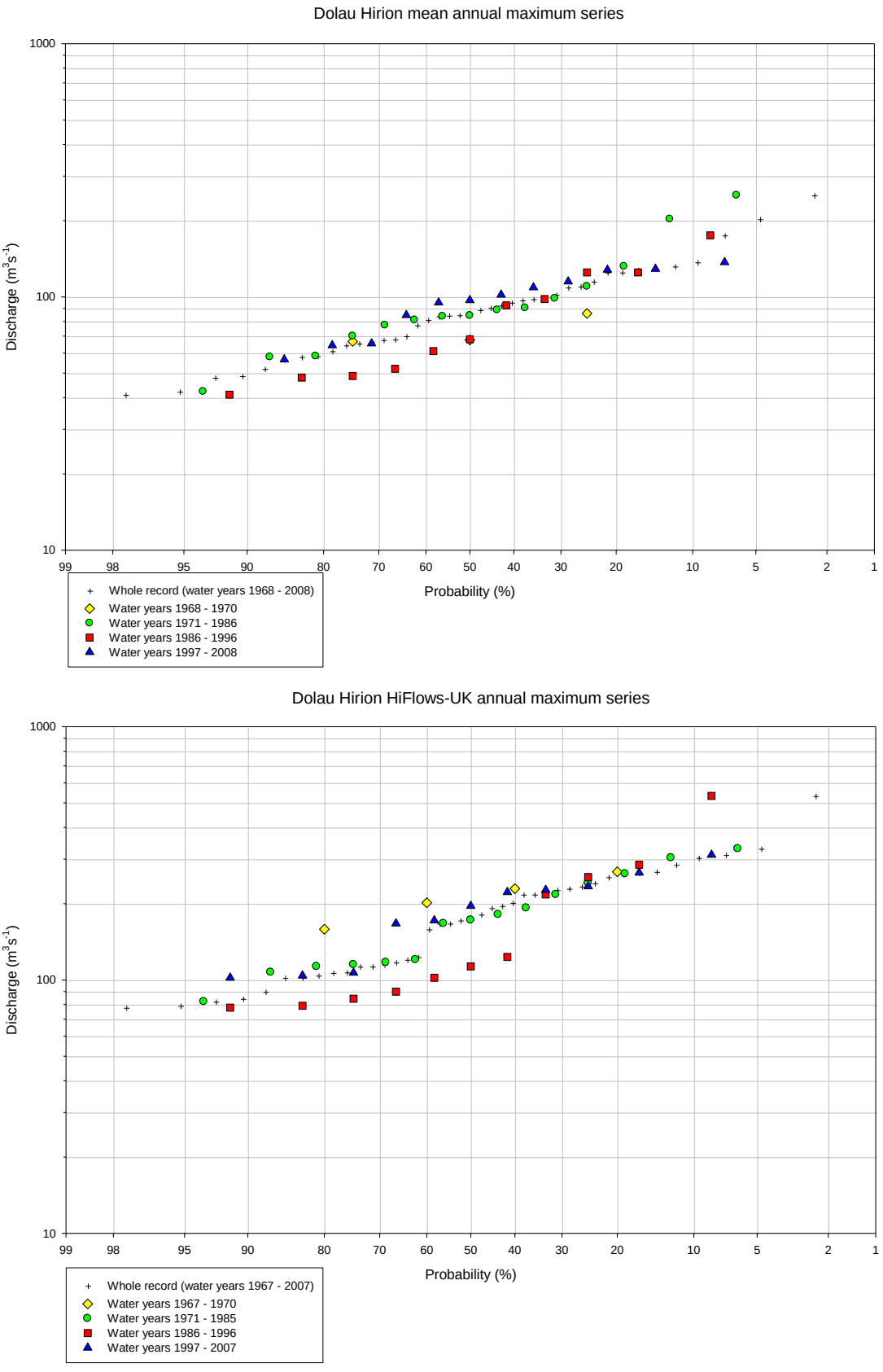

Figure 9: Flood frequency analysis of annual maximum flood data from the Dolau Hirion gauging station. Flood magnitudes are derived from daily mean flow data (top) and the HiFlows-UK archive (bottom).

The probability of such an event occurring appears elevated in the 1971-1985 and 1986-1996 periods, notably as a result of the occurrence of the single high-magnitude flood in 1987 for the 1986-1996 period. As in the flood frequency analysis on the daily mean flow data, frequent floods in the 1986-1996 period had substantially lower flood peak discharges than those in other parts of the record.

Flood frequency analysis of the small amount of daily maximum flow data from the Ty Castell gauge emphasises the lower magnitude of the flood peaks in the 1981-1983 water years as compared with those between 1999-2009. The analysis of the daily mean data indicate that flood magnitudes were generally lower in 1971-1983 and 1961-1970 than in 1999-2009, although magnitudes of the floods with the lowest annual exceedence probabilities in 1971-1983 and 1999-2009 are very similar. Flood frequency analysis of the HiFlows-UK data for this gauge emphasises the high magnitude of the 1987 flood peak. Through much of the range of annual exceedence probabilities, flood magnitudes were greater in the 1997-2007 than in the other parts of the record. In the entire record the magnitude of the flood which occurs on average in one year in ten was approximately 650 m^3s^{-1}. This value varied from between 608 m^3s^{-1} for the 1961-1970 period to c. 1000 m^3s^{-1} in the 1986-1996 period, as a result of the high magnitude of the 1987 annual maximum flood, which, according to the flood frequency analysis on the whole records, would be expected to occur in around one year in 50.

Flood frequency analysis of the annual maximum flood record derived from maximum daily flow data at the Capel Dewi gauge shows that high-magnitude flood events, with low annual exceedence probabilities, were most frequent in the 1986-1996 period. For events with higher annual exceedence probabilities, magnitudes were greater during the 1997-2009 period than in either 1981-1985 or 1986-1996.This is also apparent in the flood record derived from daily mean flow data. However, for floods with low annual exceedence probabilities, the annual maximum flood record derived from the mean daily flow data indicates that the magnitudes of such flows were greatest during the 1973-1985 period. The flood frequency analysis on the data from the HiFlows-UK data from the Capel Dewi gauge produces different results. Flood magnitudes are greatest in the 1997-2007 period for floods with annual exceedence probabilities of between 10 and 80 %. As at the Ty Castell gauging station the magnitudes of floods with annual exceedence probability of 10 % vary considerably between different parts of the record, being greatest in 1986-1997 and least in 1961-1970.

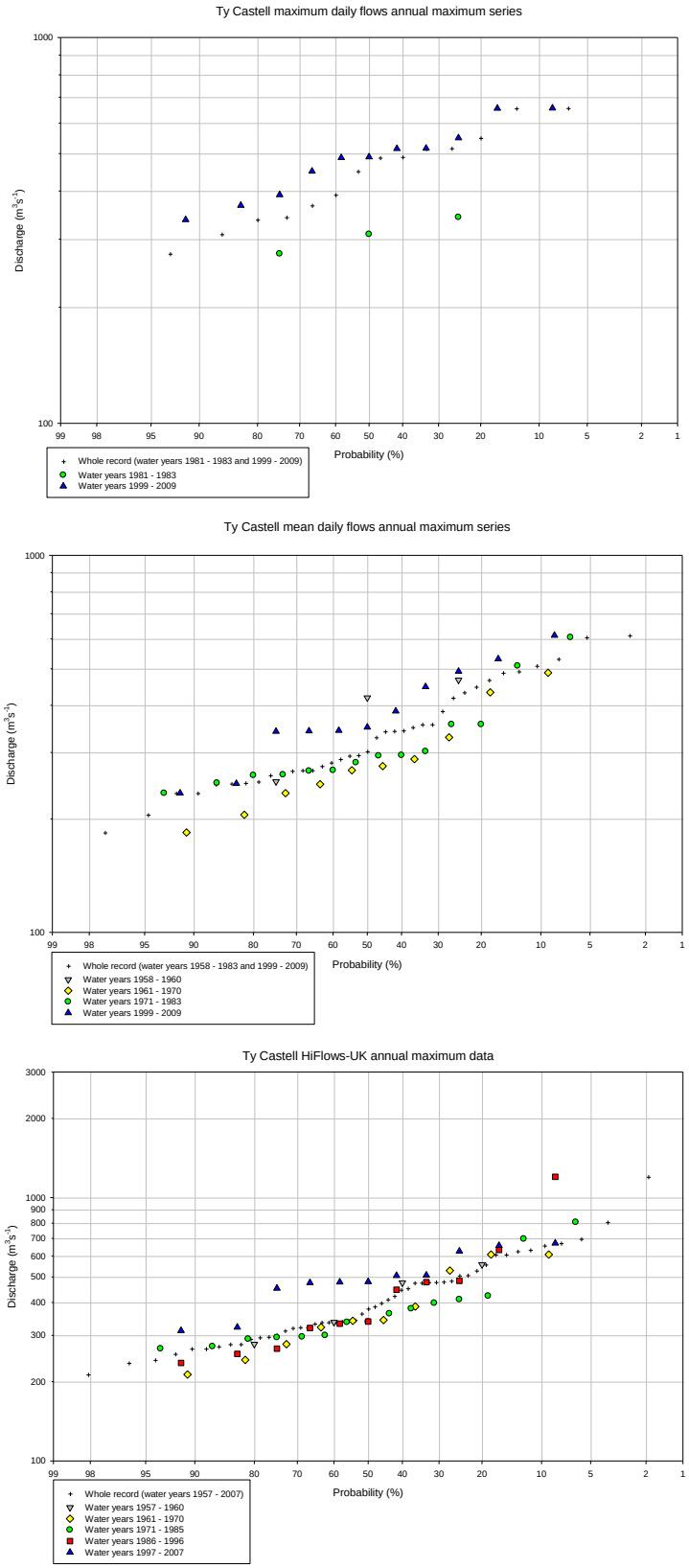

Figure 10: Flood frequency analysis of annual maximum flood data from the Ty Castell gauging station. Flood magnitudes are derived from daily maximum flow data (top), daily mean flow data (middle) and the HiFlows-UK archive (bottom).

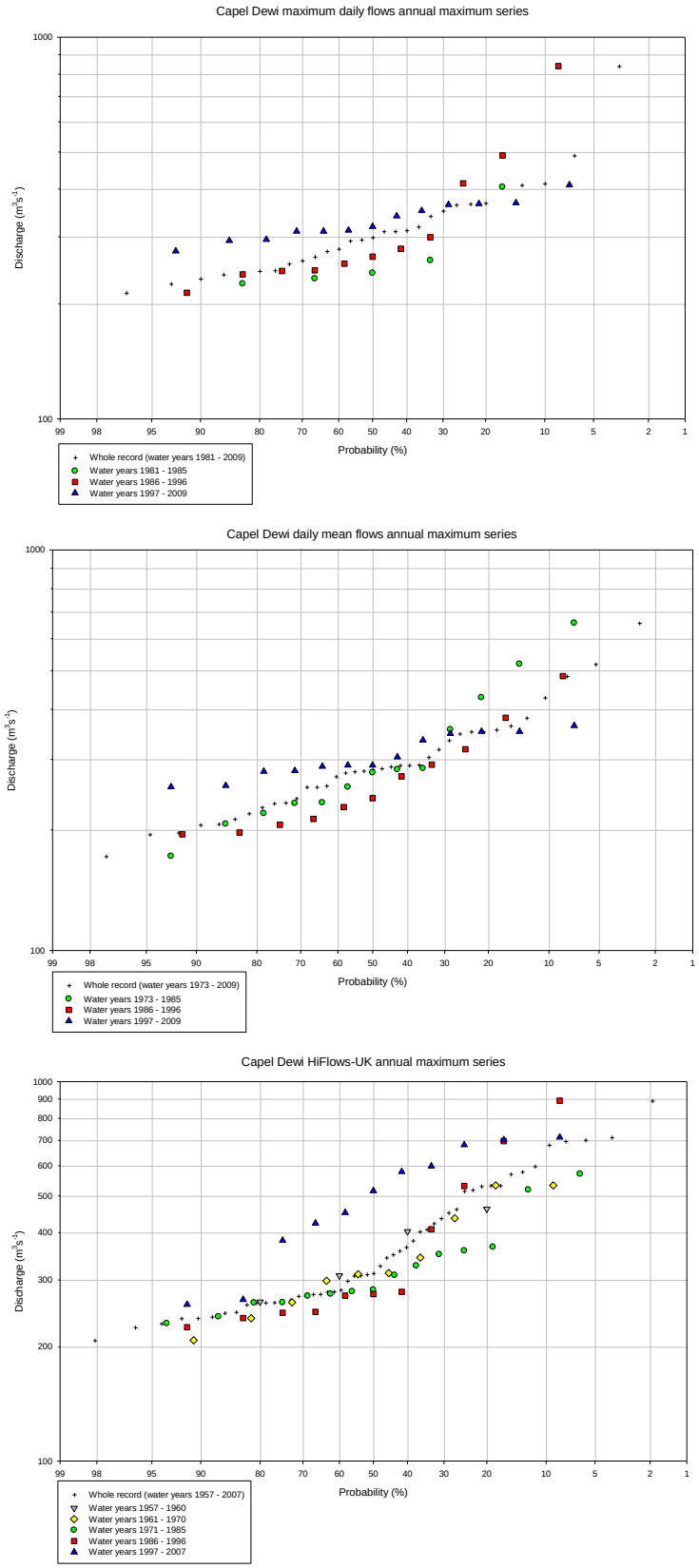

Figure 11: Flood frequency analysis of annual maximum flood data from the Capel Dewi gauging station. Flood magnitudes are derived from daily maximum flow data (top), daily mean flow data (middle) and the HiFlows-UK archive (bottom).

The results of the flood frequency analysis for the three gauges do not show any consistent relationship between annual maximum flood magnitudes and the periods of differing NAO strength on the basis of which the flood records were divided. During periods of negative NAO flood magnitudes were generally lower than those for the same annual exceedence probability in the whole record. During the period in which the winter NAO index attained strong positive values, there were a small number of particularly high-magnitude flood events, while the magnitudes of events with higher annual exceedence probabilities are similar to those in the undivided records. There are differences between the results for the periods of weakly positive winter NAO at the Ty Castell and Capel Dewi gauges, whereas the magnitudes of floods in these periods at the Dolau Hirion gauging station are similar.

3.5 Conclusion

In conclusion, the results presented in this analysis of flow gauge data for the Tywi catchment show that:

1. There may be significant differences between the magnitudes of annual maximum flood events between the different data sources for the same gauging station, notably between the flood series derived from daily maximum flow data and those from the HiFlows-UK archive, both of which provide instantaneous flood magnitudes;
2. No trends or step changes in annual maximum flood magnitudes are apparent in the records from the three gauges, but clustering of high-magnitude flood events at intervals throughout the record temporarily increases mean flood magnitudes and inter-annual variability.
3. The magnitudes of annual maximum floods with certain exceedence probabilities varies between different parts of the record. While little confidence may be placed in the accuracy of the estimates of the magnitudes of floods with low annual exceedence probabilities for such short periods, it is worth noting that the magnitudes of frequently occurring flood events (relatively high annual exceedence probabilities) may vary substantially between different periods of the record.

The short length of the records available, and the consequent limitation of the flood magnitude data in which we can place confidence to relatively high annual exceedence probabilities, provide the justification for attempts to extend the flood record in this catchment in order to better constrain predictions of future flood frequency and flood magnitude, particularly under changing climatic conditions.

4. Historical flood data

4.1 Introduction

In the previous section the systematically collected instrumental flow record was the subject of investigation. In this section the potential of the available historical data for extending the instrumental record is assessed for the Tywi catchment.

4.2 Historical flood data for the Tywi catchment

Historical flood data for the Tywi catchment have been obtained from the Chronology of British Hydrological Events database (CBHE) (Black and Law, 2004; Law *et al.*, 1998), which contained data from a range of sources. In addition, quantitative information for a single flood event which occurred prior to gauging of flows within the catchment is available from the Flood Studies Report (NERC, 1975). It is noted that information on certain floods obtained from the CBHE has since been removed from the database. No reason for this removal has yet been ascertained. However, much of the removed data had been extracted from a published source (Lewis, 1992) and is therefore included in this assessment of the available historical data.

Table 2 lists the dates of the flood events which are referred to in historical sources and also includes available information on flood magnitude. The available information suggests that the record is incomplete for the period from 1767: there are probably one or more floods of greater magnitude than that of 1831 which occurred during the 50 years prior to that date. Likewise, there is no record of the flood of 1852, although the information about the flood of 1878 imply that the flood peak magnitude in 1852 was greater than that in 1878. In addition, there is no information about the snowmelt flooding which occurred in March 1947 The only flood for which quantitative information is available is that of 1931 for which a discharge of 1270 m^3s^{-1} has been estimated, putting the peak discharge of this event close to that of the high-magnitude flood of 1987, which was the largest, by a significant margin, in the instrumental flow record.

Table 2: Historical flood events in the Tywi catchment.

Date of flood	Source	Magnitude information	Interpretation
07/02/1767	CBHE (Annual Register Vol. 10)	Largest flood in living memory	Probably the largest flood in several decades
09/02/1831	Lewis, 1992 (originally found in CBHE)	One of the largest floods in half a century (Carmarthen)	Implies occurrence of one or more larger floods in the previous 50 years
10/11/1878	CBHE (British Rainfall for 1878)	Heaviest flood for 26 years	Implies high-magnitude event occurred in 1852
28/12/1882	CBHE (British Rainfall for 1882)	Storm and heavy floods at Llandovery (observer at Llandeilo recorded that there had been no floods of any importance in the same year)	
11/02/1883	CBHE (British Rainfall for 1883)	Floods	
11/1885	CBHE (British Rainfall for 1885)	A very heavy flood	
31/08/1888	Lewis, 1992 (originally found in CBHE)	Serious flooding in Carmarthen	
13/02/1889	CBHE (British Rainfall for 1889)	Heavy flood	
25/08/1891	CBHE (British Rainfall for 1891)	Very heavy flood	
16/10/1891	Lewis, 1992 (originally found in CBHE)	Serious flood in Carmarthen " only a little less severe than that of 1894"	Peak discharge may have been close to that of 1987
14/11/1894	CBHE (Frost and Jones, 1988) and Lewis, 1992 (originally found in CBHE)	Anecdotal evidence indicates that the 1894 flood-which affected wide areas of South Britain-was also a flood of greater magnitude than is represented in the record of gauged flows (from 1958)	Peak discharge probably exceeded that of 1987
30/12/1897	Lewis, 1992 (originally found in CBHE)	Serious flood in Carmarthen	
20/01/1899	CBHE (British Rainfall for 1899)	Floods in Llandovery	
1903	CBHE (British Rainfall for 1903)	Great destruction caused by high floods	
12/11/1911	CBHE (British Rainfall for 1911)	Vale of Tywi in flood	
27/12/1924	Lewis, 1992 (originally found in CBHE)	Serious flood in Carmarthen	
20/11/1929	Lewis, 1992 (originally found in CBHE)	Water reached to within one foot of the level of the platform at Carmarthen station… The Llandeilo road was under deep water in several places	
11/1931	Flood Studies Report (NERC, 1975); CBHE (Frost and Jones, 1988)	Flood peak discharge at Ty Castell 1270 m^3s^{-1}; Evidence assembled following a major flood on the Tywi in 1931 suggests that the maximum flow on that occasion approached that experienced during the 1987 flood; an estimated flow of 1270 m^3/s is quoted in the interim Report on Floods published in 1933	Flood peak discharge for the 1987 flood at Ty Castell was first given as 1378 m^3s^{-1}; this was later revised downward to 1200 m^3s^{-1} (Environment Agency, 2010)
20/09/1946	CBHE (British Rainfall for 1946)	Floods devastated the Tywi valley	

Frost and Jones (1988) concluded that the peak discharge of the flood event of 1894 may have been greater than any flood in the instrumental record (including that of 1987), while the information collected by Lewis (1992) indicates that the flood peak discharge of the 1891 event may only have been a little lower than that of 1894. These data suggest that, since c. 1890 four flood events with a discharge similar to that of the flood of 1987 (including the 1987 flood itself) may have occurred. For those events which occurred prior to 1891 the information on flood magnitude is too limited to draw any conclusions about the length of time during which the discharges of the floods of 1891 and 1894 had not been exceeded.

4.3 Usefulness of historical flood data

Quantitative historical data, such as the estimated discharge for the 1931 at Ty Castell, are clearly the most useful for extending the instrumental flood record, particularly where rating equations exists which are suitable for converting high-magnitude flood stages to discharges. Relative magnitude information (flood X > flood Y or flood Z the largest for W years) may also potentially be incorporated into estimates of annual exceedence probabilities (cf. palaeohydrologic bounds (Levish, 2002)) where appropriate statistical techniques are available. Where magnitude data are lacking, information that a significant flood has occurred may be of use in constraining flood frequencies, although it will not be possible to attach a frequency to a particular magnitude as in conventional flood frequency analysis.

Historical flood peak data may also be used in conjunction with palaeoflood data to extend flood records. Dates of significant flood events and relative magnitudes of numbers of flood events may be used to identify events within the palaeoflood record. The dating of these events within the palaeoflood record becomes particularly secure when other dating control (for instance from radiocarbon or historical contamination) is available. Where event magnitudes are available within the historical record, floods within the palaeoflood record which occurred prior to historical recording of flood levels may be classified as having peak magnitudes ‘probably greater than flood X’ or ‘probably less than flood Y’. This type of information may also be useful in constraining the magnitude-frequency relationships of high-magnitude flood events with low annual exceedence probabilities. The type of palaeoflood information derived from floodplain sedimentary sequences, as described in the following section, is particularly suitable for

combining with historical data to constrain flood magnitude-frequency relationships in this manner.

5. Reconstruction of palaeoflood records from floodplain sediment sequences

5.1 Introduction

This section presents palaeoflood histories reconstructed using high-resolution XRF scanning of floodplain sediment sequences for the Tywi catchment at Abermarlais. The section begins with a review of the use of lithogenic element ratios as geochemical proxies and the behaviour of the three elements of interest, Zr, Ti and Rb, within sediment to demonstrate the potential of the Zr/Ti and Zr/Rb ratios for reconstructing flood histories from Jones (2007). This is followed by a description of the methods used to reconstruct the flood records, a comparison of sediment grain size with geochemical data for the two sites and presentation of the reconstructed flood records. These are then compared with proxy climate records and also with historical flood records from the Tywi catchment.

5.2 Lithogenic element ratios as grain size proxies

Inorganic element ratios are widely used in geochemical analysis of fine-grained sedimentary sequences (Boyle, 2001). The use of element ratios allows the effect of sedimentary dilution to be eliminated, when neither element is associated with the diluting fraction (Chen *et al.*, 2006; Dypvik and Harris, 2001). Element ratios have been employed in geochemical interpretation of ancient and recent marine (e.g. Calvert *et al.*, 1996; Dypvik and Harris, 2001; Land *et al.*, 1997; Scheffler *et al.*, 2006; Schneider *et al.*, 1997), lacustrine (e.g. Boyle, 2001; de Boer, 1997; Koinig *et al.*, 2003; Wolfe and Härtling, 1997) and peat bog (e.g. Shotyk *et al.*, 2001) sequences, soils and palaeosols (e.g. Driese *et al.*, 2005; Karathanasis and Macneal, 1994; Maynard, 1992), and Holocene stream sediment (e.g. Cullers, 1994). In these settings element ratios have been used as indicators of sediment provenance (e.g. Cullers, 1994; Hayashi *et al.*, 1997; Scheffler *et al.*, 2006), redox conditions (e.g. Dypvik and Harris, 2001; Koinig *et al.*, 2003), mineralogical composition (e.g. Calvert *et al.*, 1996; Schneider *et al.*, 1997), homogeneity of soil parent material (Law *et al.*, 1991; Oh and Richter, 2005), allochthonous input (e.g. de Boer, 1997; Karathanasis and Macneal, 1994; Maynard,

1992), degree of trace element enrichment (e.g. Shotyk *et al.*, 2001; Wolfe and Härtling, 1997), depositional process (e.g. Thorndycraft *et al.*, 1998) and grain size (e.g. Calvert *et al.*, 2001; Chen *et al.*, 2006; Dypvik and Harris, 2001; Oldfield *et al.*, 2003).

In a lacustrine sedimentary sequence from Petit Lac d'Annecy, France, Thorndycraft *et al.* (1998) were able to identify four major flood events using changes in the Fe/Mn ratio within the core: significantly higher values of the Fe/Mn ratio resulted from the high Fe content of minerogenic soils washed into the lake during these events. Since discrimination of flood events in fluvial sedimentary sequences is usually undertaken primarily upon the basis of grain size reversals, element ratios indicative of changes in grain size offer the potential for distinguishing between the deposits of individual flood events in fine-grained sedimentary sequences. The combination of element ratios indicative of sediment grain size changes and high-resolution core scan data provides the capability for reconstructing highly detailed records of past flood events from fluvial sedimentary sequences lacking clearly visible sediment grain size reversals.

A number of lithogenic element ratios have been used as indicators of changing grain size in various types of sediment including Si/Al (e.g. Calvert *et al.*, 1996; Calvert *et al.*, 2001), Ti/Al (e.g. Calvert *et al.*, 1996; Schneider *et al.*, 1997), Zr/Al (e.g. Calvert *et al.*, 2001; Schneider *et al.*, 1997), Zr/Ti (Oldfield *et al.*, 2003) and Zr/Rb (Chen *et al.*, 2006; Dypvik and Harris, 2001). The poor detection limits of Al and Si in Itrax XRF analyses (approximately 20 000 ppm and 10 000 ppm, respectively, using a 10 second count time; Cox Analytical Systems (no date)) means that ratios incorporating these elements were unsuitable for interpreting grain size changes from Itrax XRF data. For this reason, the application of the Zr/Ti and Zr/Rb ratios in palaeoflood reconstruction was investigated in this study.

Zr, Ti and Rb are lithogenic elements (Oldfield *et al.*, 2003; Shotyk *et al.*, 2001) which have been used as indicators of catchment erosion in lake sediment studies (e.g. de Boer, 1997; Koinig *et al.*, 2003; Wolfe *et al.*, 2005). Zr is immobile in the surficial environment (Hardardóttir *et al.*, 2001; Law *et al.*, 1991; Rose *et al.*, 1979), while Rb is slightly mobile (Rose *et al.*, 1979). Ti is often considered immobile (Hardardóttir *et al.*, 2001; Rose *et al.*, 1979), although mobility of Ti has been reported during weathering of soils, when it becomes enriched in the clay fraction (Sudom and St. Arnaud, 1971). Zr is generally insoluble (Koinig *et al.*, 2003) whereas Ti has low solubility in low temperature

aqueous solutions (Hayashi *et al.*, 1997; Law *et al.*, 1991). Zr is found principally in the heavy, weathering-resistant mineral zircon (Oh and Richter, 2005; Shotyk *et al.*, 2001; Stone *et al.*, 1997). Ti occurs in a number of different minerals with varying resistance to weathering (Law *et al.*, 1991). Rutile, ilmenite and titanite are relatively resistant to weathering (Shotyk *et al.*, 2001), although less resistant than zircon (Oh and Richter, 2005). Ti also occurs in aluminosilicates such as biotite (Shotyk *et al.*, 2001), which weathers relatively rapidly (Law *et al.*, 1991). Rb is not associated with particular minerals, but is generally dispersed in sediment, being present in minerals containing K, including K-feldspars, micas and clay minerals (Chen *et al.*, 2006). According to Dypvik and Harris (2001), Rb concentrations in sediment are frequently correlated with illite, Al_2O_3 and K_2O. Although Rb is less stable in sediments than Zr, it is not generally removed from the weathering profile until significant alteration of K-feldspars has occurred (Chen *et al.*, 2006).

During transport, by water or wind, Zr, Ti and Rb have a tendency to become concentrated in particular sediment size fractions. Zr tends to become concentrated in the coarse-grained fraction of fine-grained siliciclastic sediments, due to the resistant nature of zircon (Veldkamp and Kroonenberg, 1993), while Rb is associated with the fine-grained fraction of fine-grained siliciclastic sediments (Dypvik and Harris, 2001). Koinig *et al.* (2003) found a close correspondence between Rb concentration and variations in the <10 μm grain size fraction within a core from the Sägistalsee in Switzerland. According to Oldfield *et al.* (2003), Zr is concentrated in the silt to fine sand fractions of lacustrine sediments whereas Ti is usually enriched in the clay-size fraction. In 'average' crustal rocks Zr concentrations are higher in greywackes (302 mg kg^{-1}) than in sandstones (250 mg kg^{-1}) or shales (160 mg kg^{-1}) while Ti and Rb concentrations are higher in shales (Ti 6000 mg kg^{-1}; Rb 140 mg kg^{-1}) than in greywackes (Ti 4316 mg kg^{-1}; Rb 72 mg kg^{-1}) and sandstones (Ti 1500 mg kg^{-1}; Rb 40 mg kg^{-1}) (Reimann and de Caritat, 1998).

A number of studies have assessed quantitatively the concentration of Zr, Ti and Rb during transport in a range of environments. However, it is difficult to compare the results of these different studies due to the wide variety of grain size fractions analysed (Sutherland, 2000). Several studies have investigated the concentrations of Zr, Ti and Rb in various grain size fractions in fluvial sediment. For example, Sutherland (2000) found a statistically significant difference between the concentrations of Ti in the <63 μm

(median 2.92 %) and 63-125 μm (median 2.54 %) fractions of 121 bed sediment samples from Manoa Stream, Hawaii. Veldkamp and Kroonenberg (1993) studied the effect of grain size on the composition of sandy sediment from river terraces in the Allier and Dore catchments in the Limagne rift valley, France. They found that grain size had a significant effect on the concentration of Rb in the Allier catchment (higher Rb, lower median grain size over the range 0.2- 1.4 mm) and Ti in the Dore catchment; around 60 % of the variability in these elements was attributable to grain size (Veldkamp and Kroonenberg, 1993). Furthermore, in the Dore catchment concentrations of Zr also increased with decreasing median grain size (range 0.2-2.0 mm). In bed sediment samples from the Meurthe catchment, in the Vosges Mountains, France, Ti and Zr concentrations were higher in the <0.1 mm fraction than in the 0.1-0.3 mm and 0.3-0.5 mm fractions, and the distribution of Rb between the three fractions showed no consistent pattern (Albarède and Sehmi, 1995). Whitmore *et al.* (2004) found that the relationship between grain size and Ti, Rb and Zr in 27 New Guinea rivers draining to the Solomon Sea varied according to the underlying geology. Concentrations of these three elements tended to increase with decreasing grain size (gravel to mud) although in approximately half of cases there was no clear relationship (Whitmore *et al.*, 2004).

These studies of Zr, Ti and Rb distribution in fluvial sediments have generally focused on coarse-grained sediments, which are significantly coarser than the fine-grained overbank deposits in the Abermarlais floodplain. However, studies of variations in Zr, Ti and Rb concentrations between grain size fractions have also been undertaken in other depositional environments, such as lakes, in which finer-grained sediments predominate. For example, in samples recovered from the bed of Lake Nasser, Moalla (1997) found that Ti concentrations were highest in the 20-32 μm size fraction than in finer (<20 μm) or coarser (32-75 μm and >75 μm) fractions. Rb concentrations were found to be high in both the finest and coarsest fractions, which was attributed to the presence of Rb in clay minerals and as a detrital Rb-bearing phase in the coarse fraction (Moalla, 1997). In well-sorted surface sediments from the Skagerrak, Klaver and van Weering (1993) found that Rb was five times enriched in the clays relative to the sands whereas Zr was up to three times enriched in sands and silts compared with the clays. In a sample of modern mud from the Gulf of Mexico, Ti was found to be concentrated in the 2-10 μm fraction relative to the coarser (>10 μm) and finer (<2 μm) fractions. Rb concentrations were highest in the <2 μm fraction and considerably lower in the >10 μm fraction. Zr concentrations were highest in the >10 μm fraction and lowest

in the <2 μm fraction (Land *et al.*, 1997). Deng et al. (1998) found that Zr concentrations were highest in the silt fraction and Ti concentrations were highest in the clay-size fraction of sulphide-bearing fine-grained sediments from the Petalax district of Finland. In samples collected from the loess plateau in China, Chen at al. (2006) found that Zr concentrations were highest in the coarsest (>32 μm) fraction and lowest in the finest (<2 μm) fraction while Rb concentrations were highest in the finest fraction and lowest in the coarsest fraction.

These studies have shown that, during sediment transport, Zr tends to be concentrated in the silt and fine sand fractions of fine-grained siliciclastic sediments, while Ti is generally concentrated in intermediate size fractions and Rb is usually concentrated in the clay-size fraction. The properties of these elements means that their distribution within the sediment sequence is likely to be subject only to very minor changes after deposition and the grain size signal will be preserved (Argast and Donnelly, 1987). On this basis Zr/Ti and Zr/Rb ratios may be used as indicators of changes in the grain size of fine-grained sediments, with increasing Zr/Ti and Zr/Rb ratios indicating coarsening of the sediment and decreases in these ratios indicating sediment fining. The Zr/Ti ratio has previously been used by Oldfield *et al.* (2003) to indicate changes in lake sediment grain size in a core from Gormire Lake in northeast England while Dypvik and Harris (2001) and Chen *et al.* (2006) have used Zr/Rb ratios as an indicator of sediment size in marine sediments from the Barents Sea and loess from the loess plateau of China, respectively. Although Zr/Ti and Zr/Rb ratios have not previously been applied as grain size proxies to fluvial sediment sequences, their successful application in a range of other depositional environments suggests that they may be useful as indicators of changing grain size in the fine-grained overbank sediment sequences recovered from the Tywi catchment.

5.3 Methods

5.3.1 Geomorphological mapping and site selection

In order to select the most appropriate sites for obtaining a sedimentary flood record, and for understanding the context within which these sedimentary sequences were deposited, geomorphological maps of the sites were required. The geomorphological map for the Abermarlais site was produced from airborne LiDAR data, using the method

described by Jones *et al.* (2007), and was validated in the field during the coring programme (Figure 12).

The sites selected for sediment coring to produce the sedimentary flood records had a number of characteristics. First, they were located in palaeochannels as these topographic low points act as foci for deposition during overbank flood events through an extended period. Second, the sites were relatively close to the current channel but beyond the area of floodplain which has been reworked during the period for which historical maps and aerial photographs were available (c. 170-180 years). Parts of the floodplain which are distant from the present river channel may not have received appreciable amounts of sediment during flood events in recent centuries and consequently may produce a truncated record. Third, coring sites were selected where there was known, or expected, to be thick sequences of fine-grained, vertically-accreted floodplain deposits. In the Tywi catchment, the Abermarlais site was selected for production of a sedimentary flood record in preference to the other sites investigated because initial coring indicated that the thicknesses of fine-grained sediment were greater at this site that at the others. In addition, based on previous experience in the Severn and Dee catchments, this site was expected to be more suitable as the sediment was finer-grained (mainly silts and clays) than at other sites downstream (such as College Farm, where sedimentary sequences contained a higher proportion of sands, derived from the Old Red Sandstone, which crops out in the southern part of the catchment).

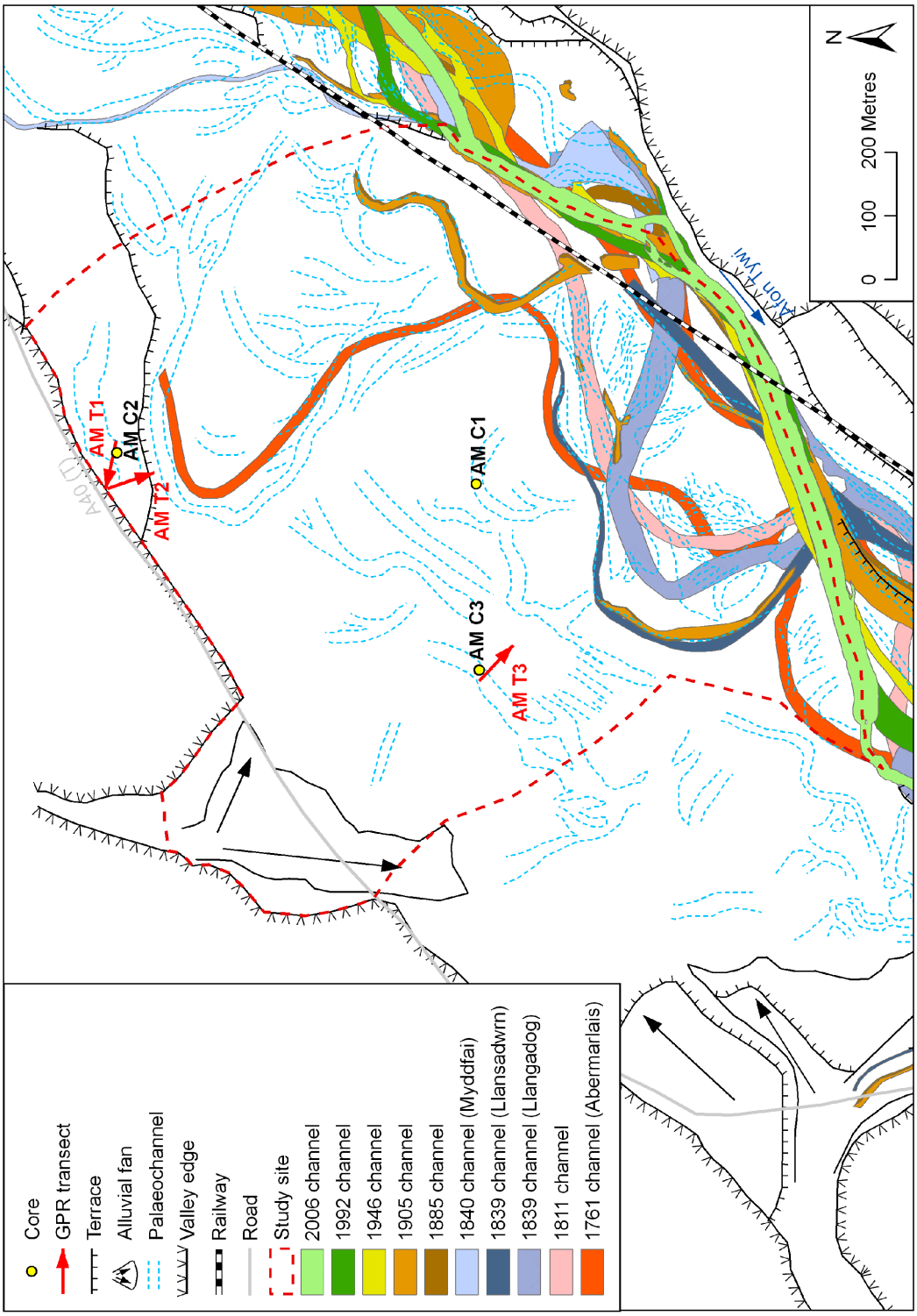

Figure 12: Geomorphological map of the Abermarlais site, showing the locations of the cores (AM C1 and AM C3) and changes in river channel position during the period for which historical maps and aerial photographs are available.

5.3.2 Sediment coring

Coring of floodplain sediment sequences was undertaken using a motorised percussion corer. Cores were collected from the Abermarlais site in June 2010. Initially, cores were collected using an open chamber gouge with an internal diameter of 75 mm. Cores were extracted in one metre sections and described in terms of colour, grain size distribution, bedding structures (e.g. imbrication) and organic matter content. Organic samples suitable for radiocarbon dating were collected where available. Subsequently, cased (50 mm diameter) cores were collected for detailed laboratory analysis. The tubes were sealed at each end immediately after extraction and were transported and stored in a horizontal position. Cased cores were initially split in half lengthwise using a circular saw to cut through the plastic tubing and either a wire or brass plates were used to split the sediment core into two halves. One half of the sample was designated as the archive half and was prepared for scanning using the Itrax core scanner and subsequently stored. The other half of the split core was sub-sampled for particle size analysis.

Five organic matter samples suitable for radiocarbon dating were recovered from the Abermarlais site: two of wood, two of charred material and one of plant material. These were sent to Beta Analytic for dating. The radiocarbon ages were calibrated using OxCal version 4 (Bronk Ramsey, 2009) and the IntCal04 calibration curve (Reimer *et al.*, 2009).

5.3.3 Itrax core scanning

The Itrax core scanner is an automated scanning instrument (Croudace *et al.*, 2006) which produces three principal types of data output: high resolution (up to 100 µm) optical and radiographic images and elemental (XRF) profiles of split sediment cores. For the production of flood records from the Abermarlais floodplain sediment sequences the Itrax core scanner was used for XRF measurements of 28 elements at 500 µm intervals using a Mo-tube operated at 30 kV and 30 mA and a 10 s exposure time. The Itrax core scanner provides XRF results as element intensities rather than element concentrations. Log-ratios of these XRF intensities were used to produce flood records. The use of log-ratios of element intensities for analysis of XRF core scan data is recommended by Weltje and Tjallingii (2008) since these are related to log-ratios of

element abundances by a linear transformation and their use minimises the possibilities of drawing erroneous conclusions from geochemical proxy data.

Gradual variations in the mean values of the log-ratios used with depth are apparent in each of the cores analysed. These trends reflect gradual changes in sediment calibre resulting from changes in floodplain-channel relationships or changes in sediment supply. Locally-weighted polynomial regression (span = 0.2) was used to fit a line describing the underlying trend in the ln(Zr/Rb) profile from each core. This line was used as a threshold for deriving the flood magnitude series. For each point the amount by which the value of ln(Zr/Rb) exceeded the threshold was calculated (giving 0 where ln(Zr/Rb) was below the threshold). This process was performed on the dara using the PeakFit v. 4.12 software.

5.3.4 Particle size analysis

Sediment grain size data were required for comparison with geochemical data to determine whether geochemical grain size proxies were suitable for use at each site. Sixteen samples each of 10 mm thickness were obtained from the two cores at Abermarlais. The sediment was sieved at 0.5 ϕ intervals down to 4 ϕ (63 μm). The silt and clay fraction was analysed using two different methods, Sedigraph and laser granulometer (Malvern Mastersizer 2000), in order to compare the results produced by the two different methods. The Sedigraph measures particle settling velocity and uses Stokes' Law to calculate sediment size distributions. The laser granulometer measures particle size using refraction of light. For this analysis a refractive index of 1.6 and an absorption of 0.01 were used.

5.4 Comparison of geochemical data with grain size data

The concentration of Zr, Ti and Rb into their characteristic size fractions during sediment transport is affected by a number of factors including geology of the source rocks and the distance and energy of sediment transport (Dypvik and Harris, 2001). For this reason it is necessary to establish, by a comparison of Zr/Ti and Zr/Rb ratios with independent grain size data, that variations in these ratios reflect changes in sediment grain size at these particular sites.

Since sediment grain size data are a type of compositional data (subject to the constant sum constraint), grain sizes was expressed as log-ratios in order to permit the application of standard statistical methods (Aitchison, 1982; Weltje and Tjallingii, 2008). It is not possible to calculate a log-ratio for two sediment grain-size fractions where the percentage of sediment in either of them is 0. For this reason, log-ratios involving fractions coarser than 3 ϕ were not calculated for either site, since sediment in this grain size range was not present in a number of the samples analysed.

Log-ratios of sediment grain size data were calculated for each pair of 0.5 ϕ size fractions smaller than 3 ϕ. The larger grain size fraction was always used as the numerator and the smaller grain size fraction as the denominator, as this should produce a positive correlation with the Zr/Ti and Zr/Rb ratios, if they are suitable for use as grain size proxies at this site, since Zr is expected to be concentrated in a coarser grain size fractions than either Ti or Rb, and therefore the Zr/Ti and Zr/Rb ratios are expected to increase with increasing grain size. A mean value of Ln(Zr/Ti) and Ln(Zr/Rb) was calculated for each subsample using the Itrax core scan data for the depth interval from which the subsample was taken. Pearson product-moment correlation was used to establish whether there was a relationship between sediment grain size and whether this relationship was of the expected form (i.e. positive). Correlation coefficients were calculated for each grain-size log-ratio with each of the two lithogenic element log-ratios. A significance level was calculated for each correlation coefficient. Correlation coefficients were calculated using grain size results from both the sedigraph and the laser granulometer, in order to determine whether there was a difference in the results according to the method used (Tables 3 to 6). Within the results tables significant correlations are highlighted. Correlations significant at the 5 % level are shaded green, those significant at the 1 % level are shaded yellow, those significant at the 0.1 % level are shaded orange and those significant at the 0.01 % level are shaded red.

Table 3: Pearson product-moment correlation between grain-size log-ratios calculated using data from the Sedigraph and Zr/Ti log-ratios for the 16 subsamples from the Abermarlais cores. The larger grain size fraction (columns) is always the dividend; the smaller (rows) is the divisor. Correlations coefficients are shown above significance levels (in brackets).

2.5-3.0	3.0-3.5	3.5-4.0	4.0-4.5	4.5-5.0	5.0-5.5	5.5-6.0	6.0-6.5	6.5-7.0	7.0-7.5	7.5-8.0	8.0-8.5	8.5-9.0	9.0-9.5	
0.0623 (0.4094)														3.0-3.5
0.0212 (-0.4689)	-0.0161 (0.5236)													3.5-4.0
0.2100 (0.2356)	-0.0674 (0.5905)	-0.1491 (0.6946)												4.0-4.5
-0.2626 (0.8371)	-0.2928 (0.8645)	-0.5709 (0.9896)	0.0918 (0.3775)											4.5-5.0
-0.2250 (0.799)	-0.2542 (0.829)	-0.5007 (0.9759)	0.1389 (0.3179)	0.3112 (0.1203)										5.0-5.5
-0.1765 (0.7434)	-0.2097 (0.7821)	-0.4246 (0.9494)	0.2661 (0.1789)	(0.08321)	0.2336 (0.1919)									5.5-6.0
-0.1260 (0.679)	-0.1573 (0.7196)	-0.3370 (0.899)	0.2763 (0.1694)	0.5313 (0.0171)	(0.03631)	(0.00192)								6.0-6.5
-0.0753 (0.6091)	-0.1064 (0.6526)	-0.2232 (0.797)	0.3301 (0.1245)	(0.00662)	0.5644 (0.0114)	(0.00083)	(0.00562)							6.5-7.0
-0.0245 (0.5359)	-0.0533 (0.5778)	-0.1005 (0.6444)	(0.09806)	(0.00376)	(0.00601)	(0.00046)	(0.00107)	(0.00125)						7.0-7.5
-0.0130 (0.519)	-0.0417 (0.5609)	-0.0737 (0.6069)	0.3584 (0.1041)	(0.00319)	(0.00552)	(0.00088)	0.6884 (0.0016)	0.6714 (0.0022)	0.2930 (0.1354)					7.5-8.0
-0.0053 (0.5078)	-0.0343 (0.5502)	-0.0546 (0.5796)	(0.09832)	(0.00255)	(0.00411)	(0.00088)	(0.00212)	(0.00255)	0.3249 (0.1098)	0.1682 (0.2667)				8.0-8.5
0.0074 (0.4891)	-0.0202 (0.5296)	-0.0207 (0.5303)	(0.09006)	(0.00254)	(0.00425)	(0.00081)	(0.00170)	(0.00199)	(0.04172)	(0.08002)	0.1672 (0.268)			8.5-9.0
0.0281 (0.4588)	0.0015 (0.4978)	0.0328 (0.4521)	(0.08087)	(0.00082)	(0.00079)	(0.00015)	(0.00029)	(0.00036)	(0.01334)	(0.03578)	(0.08236)	0.2815 (0.1455)		9.0-9.5
0.0782 (0.3867)	0.0533 (0.4222)	0.1835 (0.2481)	(0.02863)	(0.00007)	(0.00011)	(0.00003)	(0.00008)	(0.00033)	(0.01087)	(0.01705)	(0.02483)	(0.03578)	(0.09368)	9.5-10.0

Table 4: Pearson product-moment correlation between grain-size log-ratios calculated using data from the Sedigraph and Zr/Rb log-ratios for the 16 subsamples from the Abermarlais cores. The larger grain size fraction (columns) is always the dividend; the smaller (rows) is the divisor. Correlations coefficients are shown above significance levels (in brackets)

2.5-3.0	3.0-3.5	3.5-4.0	4.0-4.5	4.5-5.0	5.0-5.5	5.5-6.0	6.0-6.5	6.5-7.0	7.0-7.5	7.5-8.0	8.0-8.5	8.5-9.0	9.0-9.5	
0.1164 (0.3338)														3.0-3.5
0.0839 (0.3787)	0.0163 (0.4762)													3.5-4.0
0.3185 (0.1335)	0.0366 (0.4506)	0.0224 (0.4698)												4.0-4.5
-0.1892 (0.7586)	-0.2416 (0.8163)	-0.5127 (0.9789)	-0.1327 (0.6744)											4.5-5.0
-0.1679 (0.7328)	-0.2199 (0.7935)	-0.4769 (0.9691)	-0.0729 (0.5979)	0.1807 (0.2515)										5.0-5.5
-0.0880 (0.6271)	-0.1405 (0.698)	-0.3239 (0.8895)	0.1945 (0.2526)	0.4522 (0.0393)	0.4596 (0.0367)									5.5-6.0
-0.0265 (0.5388)	-0.0774 (0.6122)	-0.2047 (0.7766)	0.2507 (0.1937)	0.6427 (0.0036)	0.6836 (0.0018)	0.7886 (0.0001)								6.0-6.5
0.0297 (0.4565)	-0.0202 (0.5297)	-0.0750 (0.6088)	0.3101 (0.1403)	0.7071 (0.0011)	0.7536 (0.0004)	(0.00008)	0.6598 (0.0027)							6.5-7.0
0.0807 (0.3832)	0.0335 (0.451)	0.0525 (0.4235)	0.3555 (0.1061)	0.7281 (0.0007)	0.7642 (0.0003)	(0.00008)	0.7387 (0.0005)	(0.00106)						7.0-7.5
0.1003 (0.3559)	0.0533 (0.4222)	0.1020 (0.3535)	0.3648 (0.0998)	0.7512 (0.0004)	0.7806 (0.0002)	0.7992 (0.0001)	(0.00040)	(0.00048)	0.4447 (0.0422)					7.5-8.0
0.1101 (0.3424)	0.0624 (0.4093)	0.1232 (0.3247)	0.3714 (0.0955)	0.7615 (0.0003)	0.7966 (0.0001)	(0.00012)	(0.00069)	(0.00081)	(0.05411)	0.1550 (0.2833)				8.0-8.5
0.1109 (0.3413)	0.0651 (0.4054)	0.1308 (0.3146)	0.3494 (0.1104)	0.7357 (0.0006)	0.7613 (0.0003)	(0.00031)	(0.00150)	(0.00290)	(0.06127)	0.1991 (0.2299)	0.0511 (0.4255)			8.5-9.0
0.1133 (0.3381)	0.0663 (0.4037)	0.1349 (0.3092)	0.3045 (0.1449)	0.7468 (0.0004)	(0.00009)	(0.00036)	(0.00197)	(0.00713)	0.3210 (0.1127)	0.1422 (0.2997)	0.0599 (0.4128)	0.0217 (0.4682)		9.0-9.5
0.1520 (0.287)	0.1058 (0.3482)	0.2599 (0.1655)	0.3725 (0.0948)	0.7983 (0.0001)	0.8324 (0.00003)	0.7565 (0.00035)	0.6755 (0.00204)	0.5743 (0.00999)	0.3557 (0.08818)	0.2677 (0.1581)	0.2304 (0.1954)	0.2275 (0.1984)	0.2354 (0.1901)	9.5-10.0

Grain size data from the sedigraph are significantly positively correlated with both the Zr/Ti and Zr/Rb ratios. Significant positive correlations resulted between the Zr/Ti log-ratio and grain-size ratios where the dividend was between the 4.0-4.5 ϕ and the 8.5-9.0 ϕ fractions and the divisor was between the 6.0-6.5 ϕ and the 9.5-10.0 ϕ fractions. The most significant correlation was that between the log-ratio of the 5.5-6.0 ϕ fraction to the 9.5-10.0 ϕ fraction and the Zr/Ti log-ratio, which is significant at the 0.01 % level (Figure 13). Significant positive correlations between the Zr/Rb log-ratio and grain size ratios were obtained where the dividend was between the 4.0-4.5 ϕ fraction and the 7.0-7.5 ϕ fraction and the divisor was between the 5.5-6.0 ϕ and the 9.5-10.0 ϕ fractions. The most significant correlation was that between the log-ratio of the 5.0-5.5 ϕ fraction and the 9.5-10.0 ϕ fraction and the Zr/Rb log-ratio, which is significant at the 0.01 % level (Figure 14). These data suggest that sediment grain size is significantly positively correlated with both the Zr/Ti and Zr/Rb ratios and that they are therefore suitable for use as grain size proxies at the Abermarlais site.

5.5 Sedimentary flood records

For the sediment sequences recovered from each of the two cores, both Ln(Zr/Ti) and Ln(Zr/Rb) have been plotted (Figure 15). This, in effect, produces two flood records for each core. Comparison of the records produced using the two different log-ratios at each site shows that the major flood events (the largest peaks in Ln(Zr/Ti) and Ln(Zr/Rb)) usually occur at the same depths within the two records. For example, the largest peak in both Ln(Zr/Ti) and Ln(Zr/Rb) within Core AM3 occurs at 425 mm depth. It is not always the case that the peaks in each of the two records have the same relative magnitudes but, in general, where one of the records (Zr/Ti or Zr/Rb log-ratios) contains a significant peak, the other record also includes a noticeable peak at an identical or very similar depth. It is necessary to emphasize that a single flood event may produce more than one peak in either the Zr/Rb or Zr/Ti log-ratios. This is because a single major flood event may deposit a significant thickness of sediment (much greater than the measurement resolution of 0.5 mm) and that, during the course of the sediment deposition which occurs, there are likely to be temporal fluctuations in the grain size of the sediment deposited.

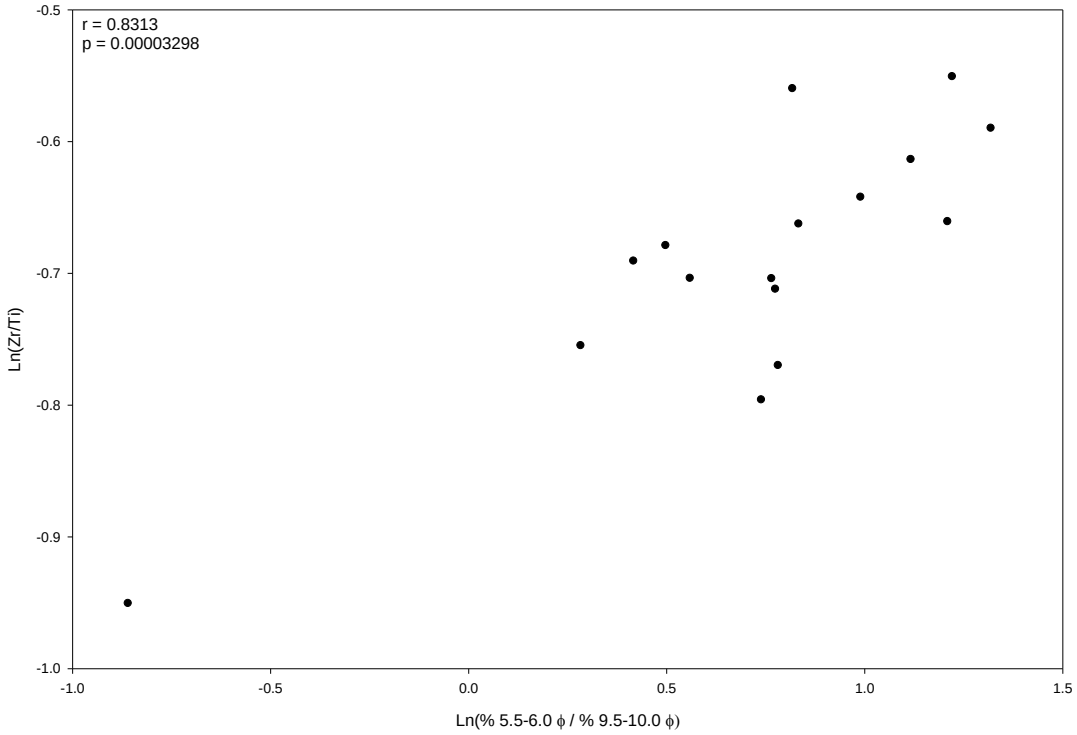

Figure 13: The most significant positive correlation between the log-ratio of Zr/Ti and sediment grain size (the ratio of the 5.5-6.0 ϕ fraction to the 9.5-10.0 ϕ fraction).

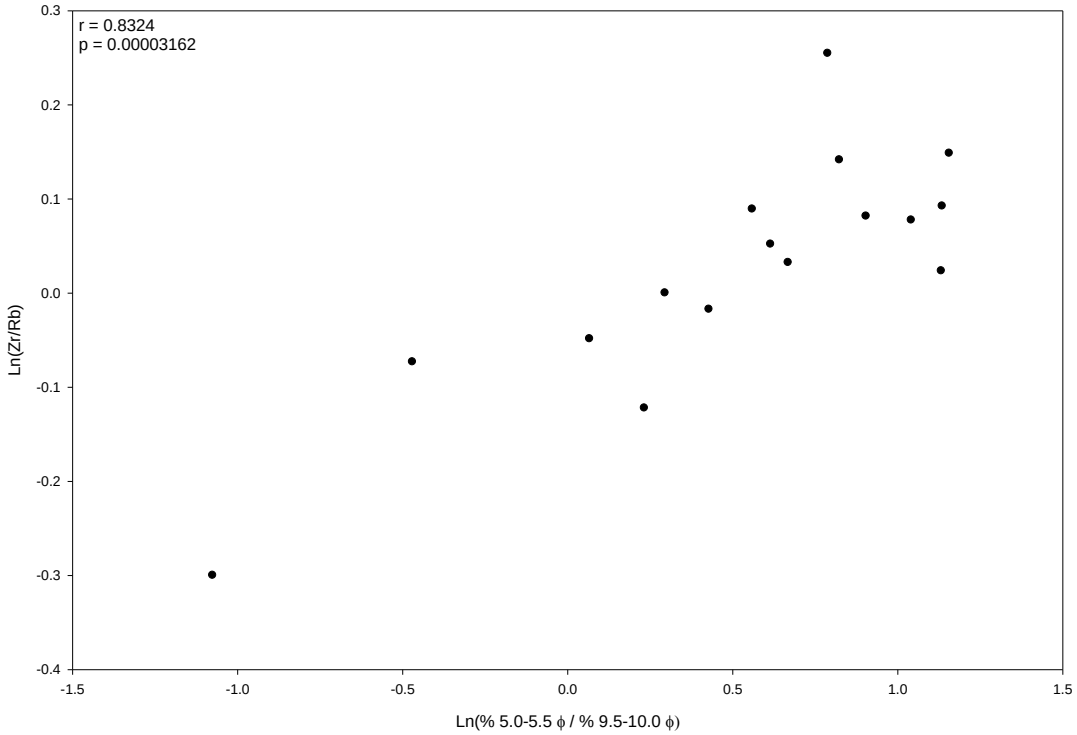

Figure 14: The most significant positive correlation between the log-ratio of Zr/Rb and sediment grain size (the ratio of the 5.5-6.0 ϕ fraction to the 9.5-10.0 ϕ fraction).

Table 5: Pearson product-moment correlation between grain-size log-ratios calculated using data from the laser granulometer and Zr/Ti log-ratios for the 16 subsamples from the Abermarlais cores. The larger grain size fraction (columns) is always the dividend; the smaller (rows) is the divisor. Correlations coefficients are shown above significance levels (in brackets).

2.5-3.0	3.0-3.5	3.5-4.0	4.0-4.5	4.5-5.0	5.0-5.5	5.5-6.0	6.0-6.5	6.5-7.0	7.0-7.5	7.5-8.0	8.5-9.0	9.0-9.5	
0.0623 (0.4094)													3.0-3.5
-0.0330 (0.5484)	-0.0821 (0.6188)												3.5-4.0
0.1294 (0.3297)	-0.0976 (0.63)	-0.0779 (0.6043)											4.0-4.5
-0.2250 (0.799)	-0.2594 (0.834)	-0.3574 (0.913)	0.2374 (0.2069)										4.5-5.0
-0.1586 (0.7213)	-0.1918 (0.7617)	-0.2494 (0.8242)	0.2486 (0.1957)	(0.06608)									5.0-5.5
-0.0962 (0.6385)	-0.1273 (0.6808)	-0.1327 (0.6879)	0.2646 (0.1803)	(0.06067)	(0.05468)								5.5-6.0
-0.0510 (0.5745)	-0.0804 (0.6163)	-0.0512 (0.5747)	0.2764 (0.1694)	(0.05572)	(0.04917)	(0.04233)							6.0-6.5
-0.0238 (0.5349)	-0.0521 (0.576)	-0.0049 (0.5072)	0.2852 (0.1615)	(0.05092)	(0.04361)	(0.03608)	(0.02943)						6.5-7.0
-0.0072 (0.5106)	-0.0350 (0.5512)	0.0226 (0.4669)	0.2953 (0.1526)	0.4367 (0.0454)	(0.03703)	(0.02849)	0.5112 (0.0215)	(0.01671)					7.0-7.5
0.0035 (0.4948)	-0.0238 (0.5349)	0.0403 (0.441)	0.3082 (0.1418)	(0.03943)	(0.03005)	(0.02085)	(0.01477)	0.5445 (0.0146)	(0.02678)				7.5-8.0
0.0095 (0.4861)	-0.0176 (0.5258)	0.0501 (0.4268)	0.3227 (0.1303)	(0.03394)	(0.02394)	(0.01499)	0.5629 (0.0116)	(0.02154)	0.3924 (0.0664)	0.2592 (0.1662)			8.0-8.5
0.0100 (0.4853)	-0.0168 (0.5247)	0.0509 (0.4257)	0.3371 (0.1193)	(0.02954)	(0.01942)	(0.01173)	(0.01444)	(0.05556)	0.2576 (0.1677)	0.1287 (0.3174)	0.0217 (0.4682)		8.5-9.0
0.0039 (0.943)	-0.0229 (0.5336)	0.0404 (0.441)	0.3510 (0.1092)	(0.02633)	(0.01664)	(0.01221)	(0.03826)	0.2568 (0.1685)	0.1092 (0.3436)	0.0047 (0.4931)	-0.0787 (0.614)	-0.1487 (0.7087)	9.0-9.5
-0.0166 (0.5244)	-0.0435 (0.5636)	0.0058 (0.4915)	(0.09785)	(0.02366)	(0.01676)	(0.03565)	0.2158 (0.2111)	0.0392 (0.4427)	-0.0577 (0.5841)	-0.1250 (0.6777)	-0.1797 (0.7473)	-0.2253 (0.7993)	-0.2624 (0.8369)	9.5-10.0

Table 6: Pearson product-moment correlation between grain-size log-ratios calculated using data from the laser granulometer and Zr/Rb log-ratios for the 16 subsamples from the Abermarlais cores. The larger grain size fraction (columns) is always the dividend; the smaller (rows) is the divisor. Correlations coefficients are shown above significance levels (in brackets).

2.5-3.0	3.0-3.5	3.5-4.0	4.0-4.5	4.5-5.0	5.0-5.5	5.5-6.0	6.0-6.5	6.5-7.0	7.0-7.5	7.5-8.0	8.0-8.5	8.5-9.0	9.0-9.5	
0.0623 (0.3338)														3.0-3.5
-0.033 (0.4513)	-0.0821 (0.5713)													3.5-4.0
0.1294 (0.201)	-0.0976 (0.4792)	-0.0779 (0.3998)												4.0-4.5
-0.2250 (0.673)	-0.2594 (0.7398)	-0.3574 (0.8194)	0.2374 (0.2492)											4.5-5.0
-0.1586 (0.5767)	-0.1918 (0.6499)	-0.2494 (0.6866)	0.2486 (0.2407)	(0.07544)										5.0-5.5
-0.0962 (0.489)	-0.1273 (0.5625)	-0.1327 (0.5342)	0.2646 (0.2316)	(0.07213)	(0.06862)									5.5-6.0
-0.0510 (0.4307)	-0.0804 (0.502)	-0.0512 (0.4344)	0.2764 (0.2306)	(0.07069)	(0.06803)	(0.06822)								6.0-6.5
-0.0238 (0.3999)	-0.0521 (0.4696)	-0.0049 (0.3851)	0.2852 (0.2344)	(0.06988)	(0.06787)	(0.06971)	0.4817 (0.0774)							6.5-7.0
-0.0072 (0.3838)	-0.035 (0.4526)	0.0226 (0.3599)	0.2953 (0.2361)	(0.06762)	(0.06541)	(0.06746)	(0.07664)	(0.08971)						7.0-7.5
0.0035 (0.3752)	-0.0238 (0.4435)	0.0403 (0.3462)	0.3082 (0.2337)	(0.06392)	(0.06093)	(0.06247)	(0.07411)	0.5445 (0.1011)	0.4908 (0.1562)					7.5-8.0
0.0095 (0.373)	-0.0176 (0.4409)	0.0501 (0.3424)	0.3227 (0.2288)	0.4675 (0.0602)	(0.05659)	(0.05871)	(0.07932)	0.5110 (0.1412)	0.3924 (0.2529)	0.2592 (0.3906)				8.0-8.5
0.0100 (0.3783)	-0.0168 (0.4462)	0.0509 (0.3504)	0.3371 (0.2237)	(0.05781)	(0.05457)	(0.06106)	0.5454 (0.109)	0.4138 (0.2428)	0.2576 (0.405)	0.1287 (0.5433)	0.0217 (0.658)			8.5-9.0
0.0039 (0.3939)	-0.0229 (0.4622)	0.0404 (0.3751)	0.3510 (0.2204)	(0.05804)	0.5336 (0.0576)	(0.08032)	0.4551 (0.2088)	0.2568 (0.43)	0.1092 (0.5835)	0.0047 (0.6852)	-0.0787 (0.7625)	-0.1487 (0.8224)		9.0-9.5
-0.0166 (0.4342)	-0.0435 (0.5036)	0.0058 (0.4406)	0.3678 (0.2229)	(0.06504)	0.5330 (0.0805)	0.4624 (0.2001)	0.2158 (0.51)	0.0392 (0.6866)	-0.0577 (0.7625)	-0.1250 (0.8115)	-0.1797 (0.85)	-0.2253 (0.8801)	-0.2624 (0.9024)	9.5-10.0

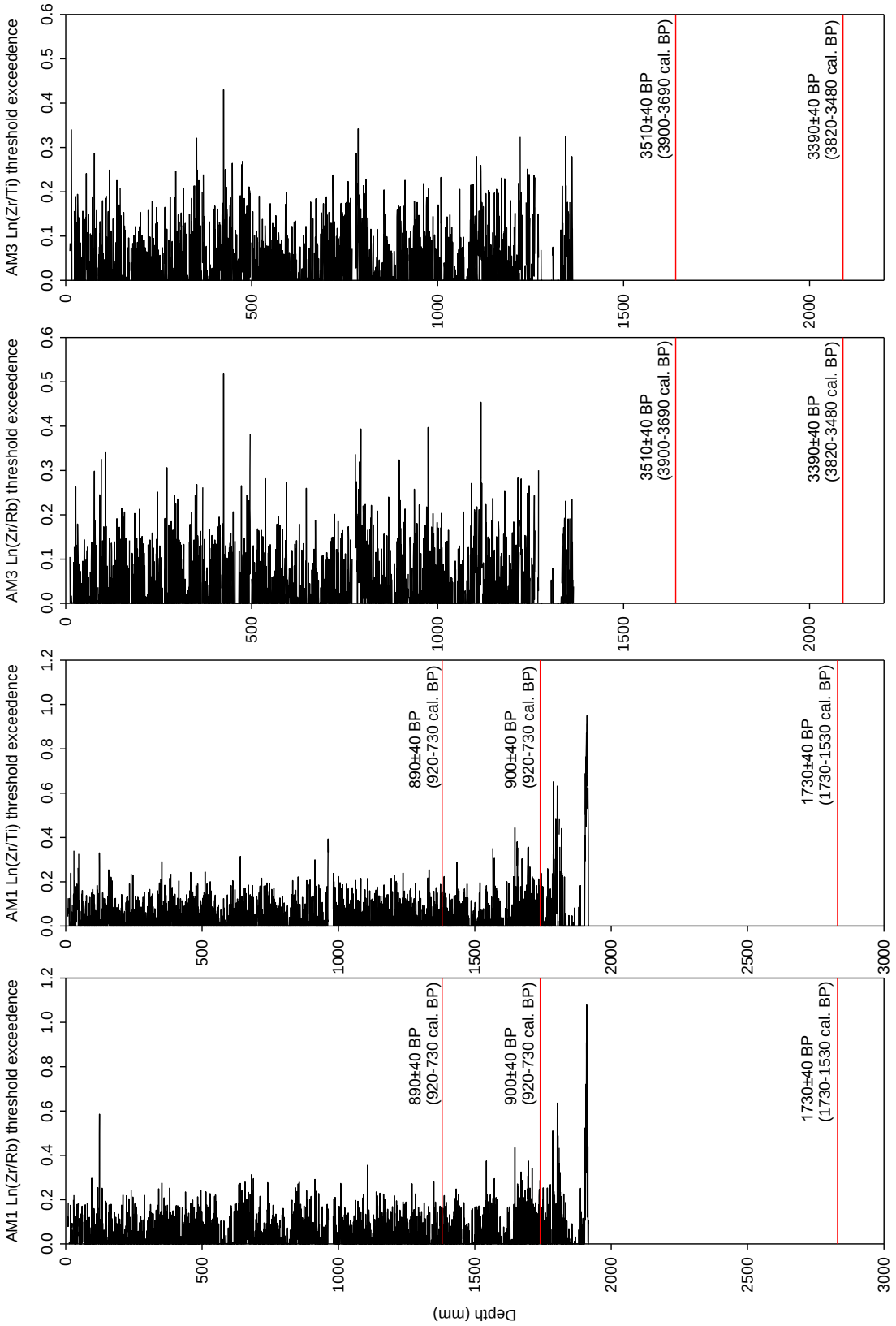

Figure 15: Flood records reconstructed using the Ln(Zr/Rb) and Ln(Zr/Ti) grain size proxies for sediment sequences recovered from Cores AM1 and AM3.

This may be caused by changes at the site during the event, related to the flow of water or deposition of sediment in the immediate vicinity of the site from which the sediment sequence was recovered, or, perhaps more likely, to variations in the calibre of sediment supplied to the site relating to fluctuations in water depth and flow velocity as the result of, for example, the arrival at different times of minor peaks generated in different sub-catchments upstream of the site or the effects of a multi-peaked rainfall event. Therefore, a cluster of peaks in the record, which occur within a few millimetres or, in some cases, a few centimetres of each other, and between which levels of the log-ratios are in general elevated above the norm, are interpreted as representing sediment deposited during the course of a single flood event.

It has thus far not been possible to determine the exact extent to which the magnitudes of peaks in the records of these geochemical grain size proxies is related to the peak discharges of the floods that deposited the sediment. The assumption is here made that a peak in either or both of ln(Zr/Rb) and ln(Zr/Ti) indicates that a major flood event has occurred. It is also assumed that, to a certain extent, the relative magnitudes of the peaks within these data series reflect the relative magnitudes of the floods that they record. However, it has not been possible to determine either the magnitude of the errors which might be expected when using the Itrax core scanner to measure the variation in elemental concentrations or the magnitude of the errors between the grain size as represented as represented by the proxy and the actual grain size or the magnitude of the errors which would result in estimating the magnitude of a flood peak discharge from the sediment which it deposited. Notwithstanding this, it has been possible to demonstrate at a site in the Severn catchment (the Roundabout, north of Welshpool), by comparison of the grain size proxy record with the occurrence of isolated individual layers of gravel within the predominantly silty sediment sequence analysed, that the coarsest layers within the sediment sequence produced the largest peaks in the grain size proxy record. The assumption that such coarse layers were deposited during flood events the magnitude of which is represented by the calibre of the sediment is an assumption which underpins the field of palaeoflood hydrology.

Both the Ln(Zr/Rb) and the Ln(Zr/Ti) grain size proxies from Core AM1 show that the largest recorded sediment grain sizes, and by implications flood discharges, are found at around 1910 mm depth and around 1800 mm depth. These two events, which occurred some time before c. 830 cal. BP, are the largest recorded in the recovered sediment sequence and may represent the largest flood events which have occurred in the reach during the past millennium. The Zr/Rb log-ratio also records a major flood event at 124 mm depth, but although a peak is present in the Ln(Zr/Ti) record it is not nearly so significant as that in the Ln(Zr/Rb) record. Consequently, although it is reasonable to conclude that a major flood event did occur at this point in time, the relative magnitude of this event in comparison with the others recorded is uncertain.

The flood record derived from the sediment sequence recovered from Core AM3 covers a significantly longer period of almost 3000 years. However, the sedimentation rate at this site during this period was much lower than that at the site of Core AM1 during the period of record with the consequence that the deposits of individual flood events are likely to be thinner at the site of Core AM3 than those at the site of Core AM1. Major flood events are recorded throughout the period of record in Core AM3, of which the peak at 425 mm depth probably represents the greatest flood discharge which has occurred within the reach during this period. Other significant flood events produced peaks in the Ln(Zr/Rb) record at 496 mm, 794 mm and 974 mm depth, while major floods recorded by the Ln(Zr/Ti) grain size proxy produced peaks at 16 mm, 352 mm, 787 mm, 1222 mm and 1345 mm depth. Of these the peaks recorded at 794 mm in the Ln(Zr/Rb) record and at 787 mm in the Ln(Zr/Ti) record probably represent the same flood event.

5.6 Conversion from depth to time

In order to compare the flood record produced using the Zr/Ti and Zr/Rb grain size proxies with other records, such as proxy records of climatic variability, it is necessary to convert the flood record from a depth scale to a timescale. A small number of dated horizons were used to convert the depth scale of the

two cores from Abermarlais to a time scale: the ground surface was assigned an age of AD2010, the year in which the cores were collected from the floodplain. Three radiocarbon-dated samples were available for Core AM1. The upper two radiocarbon samples returned ages which were very similar, as were also the calibrated ranges of these dates. Therefore, a mean depth for the two samples was calculated and the midpoint of the 2 σ ages was used in this case. The depth and mid-point of the 2 σ calibrated age range for the third sample from close to the base of the cored sequence (below the base of the sediment sequence which was recovered for laboratory analysis) was for the depth – time conversion of the basal portion of the sequence. Two radiocarbon-dated samples were available for Core AM3, both of which were recovered from horizons below those for which sediment had been recovered for laboratory analysis. The upper (and slightly older) of these two samples was used for the depth – time conversion of this core.

Linear interpolation between the dated horizons was used estimate the age of each Zr/Rb or Zr/Ti measurement within the record. For Core AM1 therefore, two different sedimentation rates were calculated, for the upper and lower portions of the core (above and below 1560 mm). For Core AM3 a single sedimentation rate was assumed for the entire period of record. The use of linear interpolation to estimate the ages of floodplain sediments between such a small number of dated horizons is not ideal. Work in other catchments, notably the upper River Severn, has revealed the extent to which floodplain sedimentation rates may vary, particularly due to anthropogenic activity in recent centuries. This includes expansion of areas used for agriculture, particularly into upland parts of the catchment and discharge of fine-grained mine waste directly to the river system. The latter is not likely to be as significant in the upper Tywi catchment as it was in the upper Severn during the 1860s to 1890s, but the extent to which agricultural activities may have affected sedimentation rates, and therefore the estimated ages of major flood events within the records from the Tywi catchment is unknown. This must be borne in mind when interpreting the result presented in the following section.

5.7 Comparison of flood records with climate proxy data

In order to compare the reconstructed flood records with regional climate proxy data, the largest peaks in each record were extracted. This was done for all peaks within the record which were more than 0.25 units above the threshold. This process was undertaken for both the ln(Zr/Ti) data and the ln(Zr/Rb) data, so that for each core two sets of peaks for the same flood may be plotted on the diagrams. In addition, floods in the modern part of the record from AM3 may also be recorded in AM1, so peaks from a small number of flood events may appear four times in the diagrams. Due to the way in which the ages of the individual flood peaks have been estimated, the same flood may have a slightly different age in the record derived from Core AM1 than in the record derived from AM3. However, the inclusion of all of the flood records in the comparison with the climate proxy data should increase the confidence in the interpretations that can be made from the comparison.

The flood records are compared here with two climate proxy data sets. The first of these is the mean age of Irish bog oaks (Leuschner *et al.*, 2002). This proxy reflects variations in regional hydroclimate. Significant rapid decreases in the mean age of Irish bog oaks is thought to indicate a rise in regional water tables which killed large numbers of bog oaks. Relatively constant mean age is achieved when similar numbers of bog oaks are germinating and dying within a particular period. Relatively dry conditions are indicated by progressive increases in the mean age of Irish bog oaks consistent with large numbers of trees aging progressively at the same time.

The results of this comparison (Figure 16) suggest that, in spite of the uncertainties about the ages of individual flood events, most high-magnitude flood occurred at times of generally low or decreasing mean age of Irish bog oaks. Relatively dry episodes, as defined by increasing or high mean age of Irish bog oaks tend to be characterised by relatively low numbers of high-magnitude flood events in the Tywi catchment. These result suggest a clustering of major flood events within the Tywi catchment during periods of generally wetter regional climate and a general lack of floods of similar magnitude in periods during which the regional climate was relatively dry.

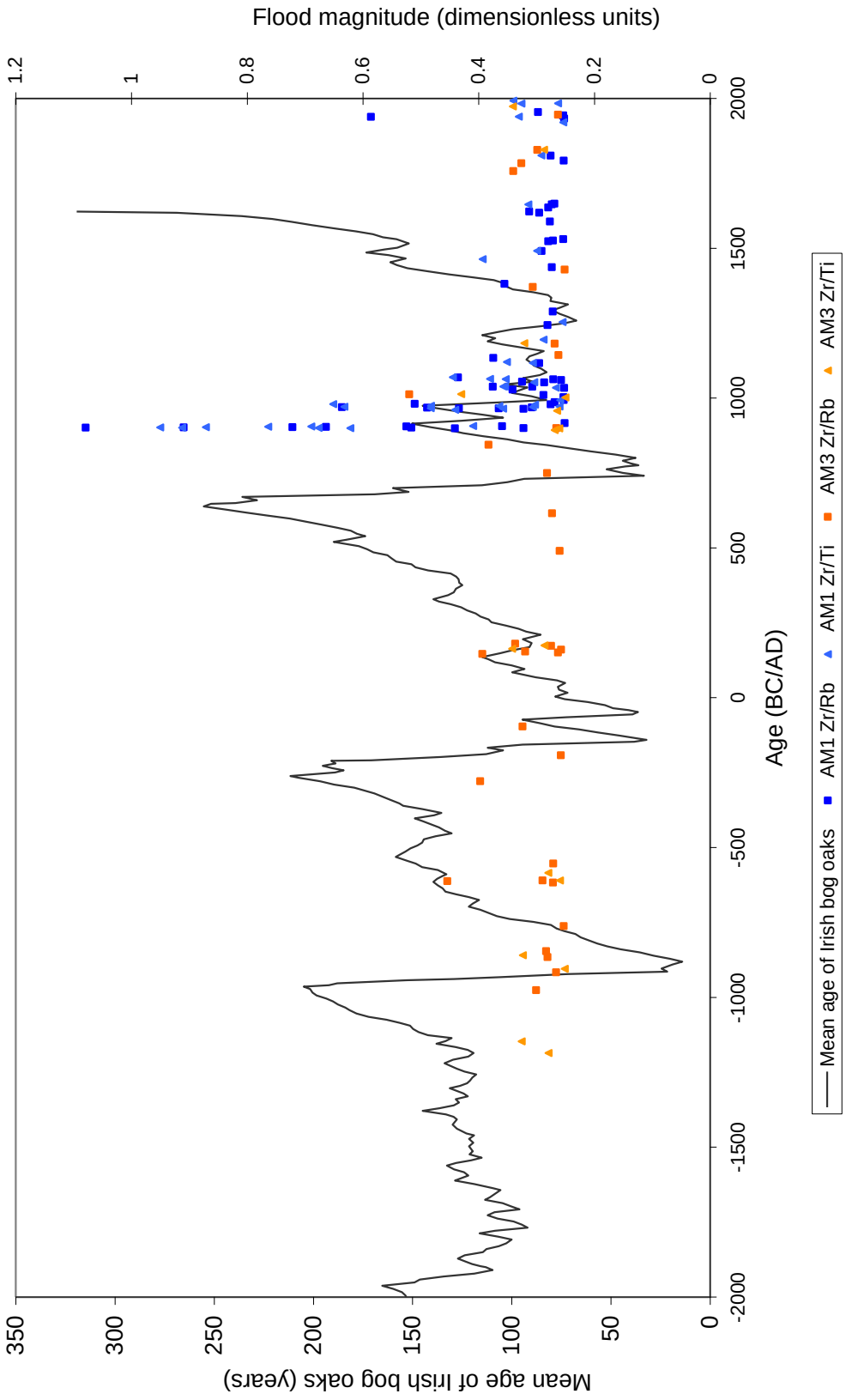

Figure 16: Flood peaks derived from the Zr/Ti and Zr/Rb records from Cores AM1 and AM3 plotted against the mean age of Irish bog oaks (Leuschner *et al.*, 2002).

The second proxy data set with which the flood records derived from the Abermarlais cores have been compared is a recent reconstruction of the North Atlantic Oscillation (NAO) by Trouet *et al.* (2009). The NAO determines the dominant circulation pattern and the location of storm tracks in the North Atlantic region, particularly in winter, the season in which the majority of floods occur in Welsh catchments. Comparison of the Abermarlais flood record with the Trouet *et al.* (2009) reconstructed NAO (Figure 17) suggests that, given the uncertainties in the estimated ages of the recorded flood events, many major floods do tend to occur during periods of weak or negative NAO, as would be expected, and that times of strongly positive NAO are characterised by relatively few major flood events. This is best illustrated by the concentration of flood events around the time of the start of the reconstructed NAO record when NAO index values were weak or negative and also by the cluster of events during the most recent period of low NAO.

5.8 Palaeoflood and historical records

The limited amount of historical flood information available for the Tywi catchment makes it difficult to compare the palaeoflood and historical flood records and, in particular, to determine whether the palaeoflood record is recording all, or the majority of, the major flood events which have occurred in the catchment during the historical period and, by implication, during earlier periods. The uncertainty in the estimated ages of the flood events, due to the relatively small number of absolute ages available for sediment sequences from which the flood record was derived and the expected non-linearity in sedimentation rates, is also an issue here. A cluster of flood events appear to have occurred during the middle and later part of the twentieth century, which may represent, among others, the major floods which occurred in 1931, 1946 and 1987. There is a noticeable gap in the latter half of the nineteenth century, however, where the flood of 1894, which was probably larger than those of 1987 and 1931, would be expected to produce a peak. The question that it is not possible at present to answer here is: is the flood of 1894 missing from the record because either the estimated age of the event is wrong and it appears earlier or later than 1894 or because, contrary to expectation, the flood failed to produce a substantial peak in either ln(Zr/Rb) or ln(Zr/Ti)?

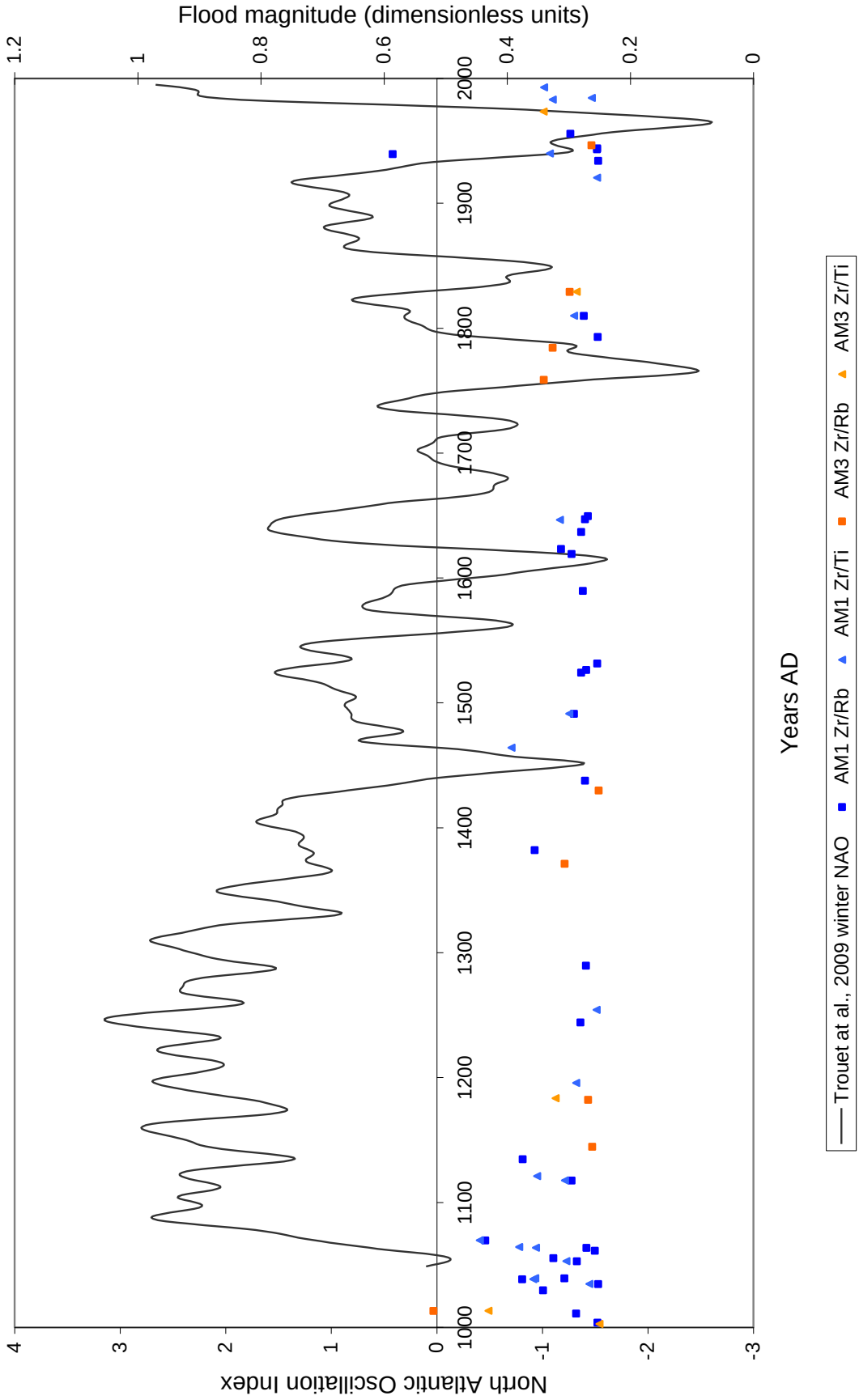

Figure 17: Flood peaks derived from the Zr/Ti and Zr/Rb records from Cores AM1 and AM3 plotted against reconstructed North Atlantic Oscillation Index (Trouet *et al.*, 2009).

Comparison of the records from the two different cores at Abermarlais does suggest that some of the major floods in the modern part of the record are recorded, as would be expected, in both cores. In some cases, however, there are substantial differences in the ages of these events as estimated in the different depth – time conversions of the two cores. It is worth noting that in the upper Severn catchment, for which a good historical flood record is available for Shrewsbury, c. 40 -50 km downstream of the location from which a sedimentary flood record was constructed, a relatively good correspondence between the historical record of flood levels and peaks in ln(Zr/Rb) has been found. The dating of the modern part of the sediment records at this site was conducted by comparison of the Pb profile with Pb mine production data, giving a more satisfactory means of depth – time conversion in the recent part of the record.

For the present, therefore, the reconstructed palaeoflood records from the Tywi at Abermarlais provide an indicator of the past flood history of the site which, with due caution used in its interpretation, may allow useful information about the long-term flood history of the reach to be gained. Further work of this nature may allow better-dated flood records to be produced in the future and may establish the extent to which the relative magnitudes of peaks in the sediment grain size proxies may be reliably used as an indicator of relative, or indeed absolute, flood magnitudes. However, it is unlikely that a significantly better historical record will be unearthed which will usefully extend or enhance that currently available with which palaeoflood data may be compared.

6 Conclusion

The results and interpretations presented in this report suggest that there is potential at the Abermarlais site for extending the available instrumental and historical flood records using high-resolution analysis of sedimentary sequences. Relationships between sediment grain size and two geochemical grain size proxies have been established for the site using the results of XRF core scanning and independent grain size data. These have been used to produce records of variation of sediment grain size, and by implication flood magnitude, at two locations in the Tywi floodplain at Abermarlais. A number of issues remain to be resolved before the full potential of such a flood record recovered from this site can be realised. Foremost among these issues is that of adequately dating such a flood and understanding how temporal variations in sediment supply, whether caused by anthropogenic activity or natural variability, may have

affected the sedimentary sequences which are used as a record of flood events. Other issues relate to interpretation of the variation in the geochemical grain size proxies, in particular, the extent to which this reflects flood peak discharges. This is a broader issue relating to the reconstruction of palaeoflood records from fine-grained floodplain sediment sequences and may be addressed by future research.

References

Aitchison, J., (1982). The statistical analysis of compositional data. *Journal of the Royal Statistical Society Series B*, **44**, 139-177.

Albarède, F. and Sehmi, K., (1995). Patterns of elemental transport in the bedload of the Meurthe River (NE France). *Chemical Geology*, **122**, 129-145.

Argast, S. and Donnelly, T. W., (1987). The chemical discrimination of clastic sedimentary components. *Journal of Sedimentary Petrology*, **57**, 813-823.

Baker, V. R., (1983). Large-scale fluvial palaeohydrology. *In*: Gregory, K. J. (ed.) *Background to Palaeohydrology*. Wiley, Chichester. 453-478.

Benito, G., Lang, M., Barriendos, M., Llasat, M. C., Frances, F., Ouarda, T., Thorndycraft, V. R., Enzel, Y., Bardossy, A., Coeur, D. and Bobee, B., (2004). Use of systematic, palaeoflood and historical data for the improvement of flood risk estimation. Review of scientific methods. *Natural Hazards*, **31**, 623-643.

Black, A. R. and Law, F. M., (2004). Development and utilization of a national web-based chronology of hydrological events. *Hydrological Sciences Journal*, **49**, 237-246.

Boyle, J. F., (2001). Inorganic geochemical methods in paleolimnology. *In*: Last, W. M. and Smol, J. P. (eds.) *Tracking Environmental Change Using Lake Sediments Volume 2: Physical and Geochemical Methods*. Kluwer Academic Publishers, Dordrecht. 83-141.

Bronk Ramsey, C., (2009). Bayesian analysis of radiocarbon dates. *Radiocarbon*, **51**, 337-360.

Calvert, S. E., Bustin, R. M. and Ingall, E. D., (1996). Influence of water column anoxia and sediment supply on the burial and preservation of organic carbon in marine shales. *Geochimica et Cosmochimica Acta*, **60**, 1577-1593.

Calvert, S. E., Pedersen, T. F. and Karlin, R. E., (2001). Geochemical and isotopic evidence for post-glacial palaeoceanographic changes in Saanich Inlet, British Columbia. *Marine Geology*, **174**, 287-305.

Cox Analytical Systems, (no date). *The Itrax Core Scanner: A Presonal Presentation*. Cox Analytical Systems, Molndal, Sweden.

Croudace, I. W., Rindby, A. and Rothwell, G., (2006). ITRAX: description and evaluation of a new multi-function X-ray core scanner. *In*: Rothwell, R. G. (ed.) *New Techniques in Sediment Core Analysis*. Geological Society of London Special Publication No. 267, London. 51-64.

Cullers, R. L., (1994). The chemical signature of source rocks in size fractions of Holocene stream sediment derived from metamorphic rocks in the Wet Mountains region, Colorado, U.S.A. *Chemical Geology*, **113**, 327-343.

de Boer, D. H., (1997). Changing contributions of suspended sediment sources in small basins resulting from European settlement on the Canadian Prairies. *Earth Surface Processes and Landforms*, **22**, 623-629.

Deng, H., Åström, M. and Björklund, A., (1998). Geochemical and mineralogical properties of sulfide-bearing fine-grained sediments in Finland. *Environmental Geology*, **36**, 37-44.

Driese, S. G., Li, Z.-H. and Horn, S. P., (2005). Late Pleistocene and Holocene climate and geomorphic histories as interpreted from a 23,000 14C yr B.P. paleosol and floodplain soils, southeastern West Virginia. *Quaternary Research*, **63**, 136-149.

Dunne, T. and Leopold, L. B., (1978). *Water in Environmental Planning*. W. H. Freeman, New York.

Dypvik, H. and Harris, N. B., (2001). Geochemical facies analysis of fine-grained siliciclastics using Th/U, Zr/Rb and (Zr+Rb)/Sr ratios. *Chemical Geology*, **181**, 131-146.

Ely, L. L., Enzel, Y., Baker, V. R. and Cayan, D. R., (1993). A 5000-year record of extreme floods and climate change in the southwestern United States. *Science*, **262**, 410-412.

Environment Agency, (2010). *HiFlows-UK* [online]. Environment Agency. Available from: http://www.environment-agency.gov.uk/hiflows/91727.aspx [Accessed: 2010].

Frost, J. R. and Jones, E. C., (1989). The October 1987 flood on the River Tywi. *In*: Institute of Hydrology (ed.) *Hydrological Data United Kingdom 1987 Yearbook*. Institute of Hydrology, Wallingford. 23-30.

Goman, M. and Leigh, D. S., (2004). Wet early to middle Holocene conditions on the upper Coastal Plain of North Carolina, USA. *Quaternary Research*, **61**, 256-264.

Gumbel, E. J., (1958). *Statistics of Extremes*. Columbia University Press, New York.

Hardardóttir, J., Geirsdóttir, Á. and Sveinbjörnsdóttir, Á. E., (2001). Seismostratigraphy and sediment studies of Lake Hestvatn, southern Iceland: implications for the deglacial history of the region. *Journal of Quaternary Science*, **16**, 167-179.

Hayashi, K.-I., Fujisawa, H., Holland, H. D. and Ohmoto, H., (1997). Geochemistry of ~1.9 Ga sedimentary rocks from northeastern Labrador, Canada. *Geochimica et Cosmochimica Acta*, **61**, 4115-4137.

Jain, S. and Lall, U., (2000). Magnitude and timing of annual maximum floods: Trends and large-scale climatic associations for the Blacksmith Fork River, Utah. *Water Resources Research*, **36**, 3641-3651.

Jain, S. and Lall, U., (2001). Floods in a changing climate: Does the past represent the future? *Water Resources Research*, **37**, 3193-3205.

Jones, A. F., Brewer, P. A., Johnstone, E. and Macklin, M. G., (2007). High-resolution geomorphological mapping of river valley environments using airborne LiDAR data. *Earth Surface Processes and Landforms*, 1574-1592.

Karathanasis, A. D. and Macneal, B. R., (1994). Evaluation of parent material uniformity criteria in loess-influenced soils of west-central Kentucky. *Geoderma*, **64**, 73-92.

Kidson, R. and Richards, K. S., (2005). Flood frequency analysis: assumptions and alternatives. *Progress in Physical Geography*, **29**, 392-410.

Klaver, G. T. and van Weering, T. C. E., (1993). Rare Earth Element fractionation by selective sediment dispersal in surface sediments: the Skagerrak. *Marine Geology*, **111**, 345-359.

Knox, J. C., (1987). Stratigraphic evidence of large floods in the upper Mississippi Valley. *In*: Mayer, L. and Nash, D. (eds.) *Catastrophic Flooding*. Allen and Unwin, Winchester, MA. 155-180.

Knox, J. C., (1993). Large increases in flood magnitude in response to modest changes in climate. *Nature*, **361**, 430-432.

Knox, J. C., (2003). North American palaeofloods and future floods: responses to climatic change. *In*: Gregory, K. J. and Benito, G. (eds.) *Palaeohydrology: Understanding Global Change*. Wiley, Chichester. 143-164.

Kochel, R. C. and Baker, V. R., (1982). Paleoflood hydrology. *Science*, **215**, 353-361.

Koinig, K. A., Shotyk, W., Lotter, A. F., Ohlendorf, C. and Sturm, M., (2003). 9000 years of geochemical evolution of lithogenic major and trace elements in the sediment of an alpine lake - the role of climate, vegetation, and land-use history. *Journal of Paleolimnology*, **30**, 307-320.

Land, L. S., Mack, L. E., Milliken, K. L. and Lynch, F. L., (1997). Burial diagenesis of argillaceous sediment, south Texas Gulf of Mexico sedimentary basin: a reexamination. *Geological Society of America Bulletin*, **109**, 2-15.

Law, F. M., Black, A. R., Scarrott, R. M. J., Miller, J. B. and Bayliss, A. C., (1998). *British Chronology of Hydrological Events* [online]. Available from: http://www.dundee.ac.uk/geography/cbhe/ [Accessed: 19.08.2006].

Law, K. R., Nesbitt, H. W. and Longstaffe, F. J., (1991). Weathering of granitic tills and the genesis of a podzol. *American Journal of Science*, **291**, 940-976.

Levish, D. R., (2002). Paleohydrologic bounds - non-exceedence information for flood hazard assessment. *In*: House, P. K., Webb, R. H., Baker, V. R. and Levish, D. R. (eds.) *Ancient Floods, Modern Hazards: Principles and Applications of Paleoflood Hydrology*. American Geophysical Union, Washington, DC. 175-190.

Lewis, R. P. W., (1992). Flooding at Carmarthen in October 1987:Historical precedents and statistical methods. *Weather*, **47**, 82-89.

Longfield, S. A. and Macklin, M. G., (1999). The influence of recent environmental change on flooding and sediment fluxes in the Yorkshire Ouse basin. *Hydrological Processes*, **13**, 1051-1066.

Macklin, M. G., Rumsby, B. T. and Newson, M. D., (1992). Historical floods and vertical accretion of fine-grained alluvium in the Lower Tyne Valley, northeast England. *In*: Billi, P., Hey, R. D., Thorne, C. R. and Tacconi, P. (eds.) *Dynamics of Gravel-bed Rivers*. Wiley, Chichester. 573-589.

Macklin, M. G. and Rumsby, B. T., (2007). Changing climate and extreme floods in the British uplands. *Transactions of the Institute of British Geographers N. S.*, **32**, 168-186.

Maynard, J. B., (1992). Chemistry of modern soils as a guide to interpreting Precambrian paleosols. *Journal of Geology*, **100**, 279-289.

Moalla, S. M. N., (1997). Physical fractionation of trace and rare earth elements in the sediments of Lake Nasser. *Talanta*, **45**, 213-221.

Moores, A. J., Passmore, D. G. and Stevenson, A. C., (1999). High resolution palaeochannel records of Holocene valley floor environments in the North Tyne Basin, Northern England. *In*: Brown, A. G. and Quine, T. A. (eds.) *Fluvial Processes and Environmental Change*. Wiley, Chichester. 283-310.

NERC, (1975). *Flood Studies Report Volume IV: Hydrological Data*. Natural Environment Research Council, London.

Oh, N.-H. and Richter, D. D., (2005). Elemental translocation and loss from three highly weathered soil-bedrock profiles in the southeastern United States. *Geoderma*, **126**, 5-25.

Oldfield, F., Wake, R., Boyle, J., Jones, R., Nolan, S., Gibbs, Z., Appleby, P., Fisher, E. and Wolff, G., (2003). The late-Holocene history of Gormire Lake (NE England) and its catchment: a multiproxy reconstruction of past human impact. *The Holocene*, **13**, 677-690.

Reimann, C. and de Caritat, P., (1998). *Chemical Elements in the Environment: Factsheets for the Geochemist and Environmental Scientist*. Springer-Verlag, Berlin.

Reimer, P. J., Baillie, M. G. L., Bard, E., Bayliss, A., Beck, J. W., Blackwell, P. G., Bronk Ramsey, C., Buck, C. E., Burr, G. S., Edwards, R. L., Friedrich, M., Grootes, P. M., Guilderson, T. P., Hajdas, I., Heaton, T. J., Hogg, A. G., Hughen, K. A., Kaiser, K. F., Kromer, B., McCormac, F. G., Manning, S. W., Reimer, R. W., Richards, D. A., Southon, J. R., Talamo, S., Turney, C. S. M., van der Plicht, J. and Weyhenmeyer, C. E., (2009). IntCal09 and Marine09 radiocarbon calibration curves, 0-50,000 years cal BP. *Radiocarbon*, **51**, 1111-1150.

Rose, A. W., Hawkes, H. E. and Webb, J. S., (1979). *Geochemistry in Mineral Exploration*. 2nd edition. Academic Press, New York.

Scheffler, K., Buehmann, D. and Schwark, L., (2006). Analysis of late Palaeozoic glacial to postglacial sedimentary successions in South Africa by geochemical proxies - Response to climate evolution and sedimentary environment. *Palaeogeography Palaeoclimatology Palaeoecology*, **240**, 184-203.

Schneider, R. R., Price, B., Müller, P. J., Kroon, D. and Alexander, I., (1997). Monsoon related variations in Zaire (Congo) sediment load and influence of fluvial silicate supply on marine productivity in the east equatorial Atlantic during the last 200,000 years. *Paleoceanography*, **12**, 463-481.

Sheffer, N. A., Rico, M., Enzel, Y., Benito, G. and Grodek, T., (2008). The palaeoflood record of the Gardon River, France: a comparison with the extreme 2002 flood event. *Geomorphology*, **98**, 71-83.

Shotyk, W., Weiss, D., Kramers, J. D., Frei, R., Cheburkin, A. K., Gloor, M. and Reese, S., (2001). Geochemistry of the peat bog at Etang de la Gruère, Jura Mountains, Switzerland, and its record of atmospheric Pb and lithogenic trace metals (Sc, Ti, Y, Zr, and REE) since 12,370 ^{14}C yr BP. *Geochimica et Cosmochimica Acta*, **65**, 2337-2360.

Stone, P., Green, P. M. and Williams, T. M., (1997). Relationship of source and drainage geochemistry in the British paratectonic Caledonides - an exploratory regional assessment. *Transactions of the Institution of Mining and Metallurgy Section B - Applied Earth Science*, **106**, B79-B84.

Sudom, M. D. and St. Arnaud, R. J., (1971). Use of quartz, zirconium and titanium as indices in pedological studies. *Canadian Journal of Soil Science*, **51**, 385-396.

Sutherland, R. A., (2000). A comparison of geochemical information obtained from two fluvial bed sediment fractions. *Environmental Geology*, **39**, 330-341.

Thorndycraft, V. R., Hu, Y., Oldfield, F., Crooks, P. R. J. and Appleby, P. G., (1998). Individual flood events detected in the recent sediments of the Petit Lac d'Annecy, eastern France. *The Holocene*, **8**, 741-746.

Veldkamp, A. and Kroonenberg, S. B., (1993). Application of bulk sand geochemistry in mineral exploration and Quaternary research: a methodological study of the Allier and Dore terrace sands, Limagne rift valley, France. *Applied Geochemistry*, **8**, 177-187.

Weltje, G. J. and Tjallingii, R., (2008). Calibration of XRF core scanners for quantitative geochemical logging of sediment cores: Theory and application. *Earth and Planetary Science Letters*, **274**, 423-438.

Whitmore, G. P., Crook, K. A. W. and Johnson, D. P., (2004). Grain size control of mineralogy and geochemistry in modern river sediment, New Guinea collision, Papua New Guinea. *Sedimentary Geology*, **171**, 129-157.

Wolfe, A. P. and Härtling, J. W., (1997). Early Holocene trace metal enrichments in organic lake sediments, Baffin Island, Arctic Canada. *Arctic and Alpine Research*, **29**, 24-31.

Wolfe, B. B., Karst-Riddoch, T. L., Vardy, S. R., Falcone, M. D., Hall, R. I. and Edwards, T. W. D., (2005). Impacts of climate and river flooding on the hydro-ecology of a floodplain basin, Peace-Athabasca Delta, Canada since AD 1700. *Quaternary Research*, **64**, 147-162.